

# Toward Deeper Understanding of Nonconvex Stochastic Optimization with Momentum using Diffusion Approximations

Tianyi Liu, Zhehui Chen, Enlu Zhou, Tuo Zhao

## Abstract

Momentum Stochastic Gradient Descent (MSGD) algorithm has been widely applied to many nonconvex optimization problems in machine learning. Popular examples include training deep neural networks, dimensionality reduction, and etc. Due to the lack of convexity and the extra momentum term, the optimization theory of MSGD is still largely unknown. In this paper, we study this fundamental optimization algorithm based on the so-called “strict saddle problem.” By diffusion approximation type analysis, our study shows that the momentum *helps escape from saddle points*, but *hurts the convergence within the neighborhood of optima* (if without the step size annealing). Our theoretical discovery partially corroborates the empirical success of MSGD in training deep neural networks. Moreover, our analysis applies the martingale method and “Fixed-State-Chain” method from the stochastic approximation literature, which are of independent interest.

## 1 Introduction

Nonconvex stochastic optimization naturally arises in many machine learning problems. Taking training deep neural networks as an example, given  $n$  samples denoted by  $\{(x_i, y_i)\}_{i=1}^n$ , where  $x_i$  is the  $i$ -th input feature and  $y_i$  is the response, we solve the following optimization problem,

$$\min_{\theta} \mathcal{F}(\theta) := \frac{1}{n} \sum_{i=1}^n \ell(y_i, f(x_i, \theta)), \quad (1.1)$$

where  $\ell$  is a loss function,  $f$  denotes the decision function based on the neural network, and  $\theta$  denotes the parameter associated with  $f$ .

Among existing algorithms for solving (1.1), the most popular one is the Momentum Stochastic Gradient Descent (MSGD). Specifically, at the  $t$ -th iteration, we uniformly sample  $i$  from  $(1, \dots, n)$ . Then, we take

$$\theta^{(t+1)} = \theta^{(t)} - \eta \nabla \ell(y_i, f(x_i, \theta^{(t)})) + \mu(\theta^{(t)} - \theta^{(t-1)}), \quad (1.2)$$

where  $\eta$  is the step size parameter and  $\mu \in [0, 1)$  is the parameter for controlling the momentum. Note that when  $\mu = 0$ , (1.2) is reduced to the vanilla Stochastic Gradient Descent (VSGD).

Although SGD-type algorithms have demonstrated significant empirical successes for training deep neural networks. Due to the lack of convexity, their convergence properties for nonconvex optimization are still largely unknown. For VSGD, existing literature shows that it is guaranteed to converge to a first-order optimal solution (i.e., stationary point  $\nabla\mathcal{F}(\theta) = 0$ ) under some general regularity conditions for nonconvex optimization.

The theoretical investigation of MSGD is even more limited than that of VSGD. The momentum in (1.2) has been observed to significantly accelerate computation in practice. To the best of our knowledge, we are only aware of Ghadimi and Lan (2016) in existing literature, which shows that MSGD is guaranteed to converge to a first-order optimal solution. Their analysis, however, does not justify the advantage of the momentum in MSGD over VSGD.

The major difficulty for analyzing MSGD is the complex nonconvex optimization landscape in high dimensions. Some recent research proposes to understand VSGD for nonconvex optimization based on relatively simple examples in machine learning such as the matrix and tensor factorization. These simple problems enjoy the “strict saddle” property (i.e., the objective function has negative curvatures around all saddle points). For example, Chen et al. (2017) shows that for eigenvalue problems, the nonconvex optimization landscape contains the following three regions:

- $\mathcal{R}_1$ : The region containing the neighborhood of all strict saddle points with negative curvatures.
- $\mathcal{R}_2$ : The region including the set of points whose gradient has sufficiently large magnitude.
- $\mathcal{R}_3$ : The region containing the neighborhood of all global optima with a positive curvature along a certain direction.

They further use the simple Infinitesimal Perturbed Analysis to analyze the algorithmic behavior of VSGD in each region and provide global convergence rates based on the diffusion approximation under certain regularity conditions. For another example, Li et al. (2016) study the ICA problem and use the diffusion process to help understand the global dynamics of VSGD. These results, though simplified, help us gain deeper understanding of nonconvex stochastic optimization for VSGD (e.g., the role of noise).

In this paper, we propose to investigate Momentum SGD for solving nonconvex optimization problems. Specifically, we consider the same eigenvalue problem as in Chen et al. (2017). We are interested in characterizing the algorithmic behavior of MSGD and answering a natural and fundamental question:

*What is the role of the momentum?*

Our analysis is also based on the diffusion approximation of stochastic optimization, which is a powerful tool in applied probability. Specifically, we prove asymptotically the solution trajectory of MSGD converges weakly to the solution of an appropriately constructed ODE/SDE, and this solution can provide intuitive characterization of the algorithmic behavior. We remark here the major technical challenge is to prove the weak convergence of the trajectory sequence. This is

because the Infinitesimal Perturbed Analysis used in [Chen et al. \(2017\)](#); [Li et al. \(2016\)](#) is not applicable here due to the complex structure of MSGD. Instead, we apply the martingale method and “Fixed-State-Chain” method from the stochastic approximation literature ([Kushner and Yin, 2003](#)). To the best of our knowledge, we are the first to apply these powerful methods to analyze MSGD.

Our result shows the momentum can play different but important roles in the three regions mentioned above:

- *The momentum helps escape from the neighborhood of saddle points ( $\mathcal{R}_1$ ):* In this region, since the gradient diminishes, the variance of the stochastic gradient dominates the algorithmic behavior. Our analysis indicates that the momentum greatly increases the variance and perturbs the algorithm more violently. Thus, it becomes harder for the algorithm to stay around saddle points. In addition, the momentum also encourages more aggressive exploitation, and in each iteration, the algorithm makes more progress along the descent direction by a factor of  $\frac{1}{1-\mu}$ , where  $\mu$  is the momentum parameter.
- *The momentum helps evolve toward global optima in the non-stationary region ( $\mathcal{R}_2$ ):* In this region, the variance of the stochastic gradient can be neglected due to the larger magnitude of the gradient. At the same time, with the help of the momentum, the algorithm makes more progress along the descent direction. Thus, the momentum can accelerate the algorithm in this region by a factor of  $\frac{1}{1-\mu}$ .
- *The momentum hurts the convergence within the neighborhood of global optima ( $\mathcal{R}_3$ ):* Similar to  $\mathcal{R}_1$ , the gradient dies out, and the variance of the stochastic gradient dominates. Since the momentum increases the variance, it is harder for the algorithm to enter the small neighborhood. To this respect, the momentum hurts in this region.

This characterization has a profound impact and can help explain some phenomena observed when training deep neural networks. There have been some empirical observations and theoretical results ([Choromanska et al., 2015](#)) showing that saddle points ( $\mathcal{R}_1$ ) are the major computation bottleneck, and the SGD algorithm usually spends most of the time traveling along regions similar to  $\mathcal{R}_1$  and  $\mathcal{R}_2$ . Since the momentum helps in both regions, we can find in practice MSGD performs better than SGD. In addition, from our analysis, the momentum hurts convergence within  $\mathcal{R}_3$ . However, we can address this problem by decreasing the step size or the momentum.

We further verify our theoretical findings through numerical experiments on training a ResNet-18 deep neural network using the CIFAR-100 dataset. The experimental results show that the algorithmic behavior of MSGD is consistent with our analysis. Moreover, we observe that with a proper initial step size and a proper step size annealing process, MSGD eventually achieves better generalization accuracy than that of VSGD in training neural networks.

Several recent results are closely related to our work. In [Li et al. \(2017\)](#), the authors apply techniques from the SDE numerical solutions to derive the so-called Stochastic Modified Equations for VSGD. However, this result is based on the assumption that the drift term in the SDE is bounded,

which is actually not satisfied when we have the momentum. Thus, we cannot naively generalize it to MSGD. Many other papers consider different kinds of accelerated SGD in the convex case by the SDE approximation. For example, Wang (2017) obtain a second-order SDE for the stochastic version of Nesterov Accelerated Gradient (NAG). Krichene and Bartlett (2017) use differential equations to study the dynamics of accelerated SGD in solving smooth convex problems. Because of the lack of convexity, our problem is different and technically challenging.

The rest of the paper is organized as follows: Section 2 introduces our motivating example – Streaming PCA and our proposed stochastic generalized Hebbian algorithm with momentum; Section 3 analyzes the global dynamics of our proposed algorithm based diffusion approximations; Section 4 analyzes the local dynamics of our proposed algorithm based diffusion approximations; Section 5 discusses the connection between our theory and training deep neural networks; Section 6 presents the numerical experiments on both streaming PCA and training deep neural networks to support our proposed theory; Section 7 makes some further discussions on our experimental results and future work; The appendix presents all technical details.

**Notations:** For  $1 \leq i \leq d$ , let  $e_i = (0, \dots, 0, 1, 0, \dots, 0)^T$  ( $i$ -th dimension equals to 1, others 0) be the standard basis in  $\mathbb{R}^d$ . Given a vector  $v = (v^{(1)}, \dots, v^{(d)})^\top \in \mathbb{R}^d$ , we define the vector norm:  $\|v\|^2 = \sum_j (v^{(j)})^2$ . The notation *w.p.1* is short for with probability one,  $B_t$  is the standard Brownian Motion in  $\mathbb{R}^d$ , and  $\mathbb{S}$  denotes the sphere of the unit ball in  $\mathbb{R}^d$ , i.e.,  $\mathbb{S} = \{v \in \mathbb{R}^d \mid \|v\| = 1\}$ .  $\dot{F}$  denotes the derivative of the function  $F(t)$ .

## 2 Momentum SGD for Streaming PCA

We study MSGD through the streaming PCA problem. Specifically, given a streaming data set  $\{X_k\}_{k=1}^\infty$  drawn independently from some unknown zero-mean distribution  $\mathcal{D}$ , we consider the following problem

$$\max_v v^T \mathbb{E}_{X \sim \mathcal{D}}[XX^T]v \quad \text{subject to} \quad v^T v = 1. \quad (2.1)$$

Note that (2.1) is essentially an eigenvalue problem, and the global optimum is the leading eigenvector. (2.1) is also well known as a nonconvex optimization problem, but with several nice computational structures. The global optimum can be obtained in polynomial time. For example, we can apply the power method to solve (2.1) with a linear convergence guarantee under certain regularity conditions. However, it is a batch algorithm and requires access to all data points. Thus, the power method cannot be applied to streaming PCA (or when the sample size is super large). Instead, we can apply SGD-type algorithms, such as Oja’s Algorithm (Krasulina, 1970; Oja and Karhunen, 1985; Oja, 1992) and Stochastic Generalized Hebbian Algorithm Sanger (1989). These methods achieve sub-linear convergence with cheap computation cost per iteration.

The optimization landscape of (2.1) has been well studied. For notational simplicity, denote  $\Sigma = \mathbb{E}[XX^T]$ . Before we proceed, we impose the following assumption on  $\Sigma$ :

**Assumption 1.** *The covariance matrix  $\Sigma$  is positive definite with eigenvalues*

$$\lambda_1 > \lambda_2 \geq \dots \geq \lambda_d > 0$$

*and associated normalized eigenvectors  $v^1, v^2, \dots, v^d$ .*

Under this assumption, [Chen et al. \(2017\)](#) have shown that the eigenvectors

$$\pm v^1, \pm v^2, \dots, \pm v^d$$

are all the stationary points for problem (2.1) on the unit sphere  $\mathbb{S}$ . Moreover, the eigen-gap assumption ( $\lambda_1 > \lambda_2$ ) guarantees that the global optimum  $v^1$  is identifiable up to sign change. Meanwhile,  $v^2, \dots, v^{d-1}$  are  $d - 2$  strict saddle points, and  $v^d$  is the global minimum ([Panageas and Piliouras, 2016](#)).

Here we are interested in streaming PCA, since some of its computational structures, such as saddle points, also appear in many other nonconvex problems. For example, training deep neural networks (DNNs) has been notorious for its complex optimization landscape. However, some recent empirical evidences and theoretical results suggest that the saddle point is also one of the crucial computational bottlenecks for training DNNs ([Choromanska et al., 2015](#); [Dauphin et al., 2014](#)). Thus, we expect that understanding the algorithmic behavior around saddle points for PCA could lead us to more theoretical insights on training DNNs.

Given the optimization landscape of (2.1), we have already understood the behavior of VSGD (Oja’s and SGHA algorithms) for solving streaming PCA problems ([Chen et al., 2017](#)). For MSGD, however, the additional momentum term makes the algorithmic analysis much more challenging. The role of the momentum demands further empirical and theoretical investigations. In this paper, we focus on analyzing MSGD for solving streaming PCA. Specifically, we consider the Stochastic Generalized Hebbian Algorithm (SGHA). Recall that we are given a streaming data set  $\{X_k\}_{k=1}^\infty$  drawn independently from some unknown zero-mean distribution  $\mathcal{D}$ . At the  $k$ -th iteration, SGHA takes

$$\begin{aligned} v_{k+1} &= v_k + \eta(X_k X_k^T v_k - v_k^T X_k X_k^T v_k v_k) \\ &= v_k + \eta(\Sigma_k v_k - v_k^T \Sigma_k v_k v_k), \end{aligned} \tag{2.2}$$

where  $\Sigma_k = X_k X_k^T$ . The detailed derivation can be found in [Chen et al. \(2017\)](#). Moreover, [Bonnabel \(2013\)](#) show that  $X_k X_k^T v_k - v_k^T X_k X_k^T v_k v_k$  is essentially the stochastic approximation of the manifold gradient on the unit sphere, since when  $v \in \mathbb{S}$ , we have

$$v^T (X X^T v - v^T X X^T v v) = 0,$$

which means that  $X X^T v - v^T X X^T v v$  is tangent to  $v$ . We then further propose a Momentum SGHA by adding the Polyak’s Momentum term  $\mu(v_k - v_{k-1})$ :

$$v_{k+1} = v_k + \mu(v_k - v_{k-1}) + \eta(X_k X_k^T v_k - v_k^T X_k X_k^T v_k v_k), \tag{2.3}$$

where  $\mu \in [0, 1)$  is the tuning parameter. When  $\mu = 0$ , (2.3) is reduced to (2.2). In the following analysis, we denote SGHA as SGD and Momentum SGHA as MSGD.

### 3 Analyzing Global Dynamics by ODE

We first analyze the global dynamics of Momentum SGD (MSGD) based on a diffusion approximation framework. Roughly speaking, by taking  $\eta \rightarrow 0$ , the continuous-time interpolation of the trajectory  $\{v_k\}_{k=0}^\infty$ , which can be treated as a stochastic process with Càdlàg paths (right continuous and have left-hand limits), becomes a continuous stochastic process. For MSGD, this continuous process follows an ODE with an analytical solution. Such a solution helps us understand how the momentum affects the global dynamics. We remark that  $\mu$  is a *fixed constant* in our analysis.

More precisely, define the continuous-time interpolation  $V^\eta(\cdot)$  of the solution trajectory of the algorithm as follows: For  $t \geq 0$ , set  $V^\eta(t) = v_k^\eta$  on the time interval  $[k\eta, k\eta + \eta)$ . Throughout our analysis, similar notations apply to other interpolations (e.g.  $H^\eta(t)$ ,  $U^\eta(t)$ ). We then answer the following question:

*Does the solution trajectory sequence  $\{V^\eta(\cdot)\}_\eta$  converge weakly when  $\eta$  goes to zero?  
If so, what is the limit?*

This question has been studied for SGD in [Chen et al. \(2017\)](#). They use the Infinitesimal Perturbed Analysis (IPA) technique to show that under some regularity conditions,  $V^\eta(\cdot)$  converges weakly to a solution of the following ODE:

$$\dot{V}(t) - (\Sigma V - V^T \Sigma V) = 0.$$

This method, however, cannot be applied to analyze MSGD due to the additional momentum term. Here, we explain why this method fails. We rewrite the algorithm (2.3) as

$$\delta_{k+1} = \mu\delta_k + \eta[\Sigma_k v_k - v_k^T \Sigma_k v_k], \quad v_{k+1} = v_k + \delta_{k+1}.$$

One can easily check  $(\delta_k, v_k)$  is Markovian. To apply IPA, the infinitesimal conditional expectation (ICE) must converge to a constant. However, the ICE for MSGD, which can be calculated as follows:

$$\frac{\mathbb{E}[\delta_{k+1} - \delta_k | \delta_k, v_k]}{\eta} = \frac{(\mu - 1)\delta_k}{\eta} + [\Sigma v_k - v_k^T \Sigma v_k],$$

goes to infinity (blows up). Thus, we cannot apply IPA.

To address this challenge, we provide a new technique to prove the weak convergence and find the desired ODE. Roughly speaking, we first prove rigorously the weak convergence of the trajectory sequence. Then, with the help of the martingale theory, we find the ODE. For self-containedness, we provide a summary on the pre-requisite weak convergence theory in [Appendix A](#).

Before we proceed, we impose the following assumption on the problem:

**Assumption 2.** *The data points  $\{X_k\}_{k=1}^\infty$  are drawn independently from a distribution  $\mathcal{D}$  defined on  $\mathbb{R}^d$ , such that:*

$$\mathbb{E}[X] = 0, \mathbb{E}[XX^T] = \Sigma, \|X\| \leq C_d,$$

where  $C_d$  is a constant (possibly dependent on  $d$ ).

This uniformly boundedness assumption can actually be relaxed to the boundedness of the  $(4 + \delta)$ -th-order moment ( $\delta > 0$ ) with a careful truncation argument. The proof, however, will be much more involved and beyond the scope of this paper. Thus, we use the uniformly boundedness assumption for convenience.

We first show the trajectory sequence  $\{V^\eta(\cdot)\}_\eta$  converges weakly. Let  $D^d[0, \infty)$  be the space of  $\mathbb{R}^d$ -valued functions which are right continuous and have left-hand limits for each dimension. By Prokhorov's Theorem A.3 (in Appendix A), we need to prove tightness, which means  $\{V^\eta(\cdot)\}_\eta$  is bounded in probability in space  $D^d[0, \infty)$ . This can be proved by Theorem A.5 (in Appendix A) which requires the following two conditions: (1)  $v_k$  must be bounded in probability for any  $k$  uniformly in step size  $\eta$ ; (2) The maximal discontinuity (the largest difference between two iterations, i.e.,  $\max_k \{v_{k+1} - v_k\}$ ) must go to zero as  $\eta$  goes to 0.

**Remark 3.1.** *These two conditions come from the special metric we use in the space  $D^d[0, \infty)$ . It is called "Skorokhod metric" and can measure not only the function value but also the continuity. See more details in Sagitov (2013).*

The next lemma proves that these two conditions hold for our algorithm.

**Lemma 3.2.** *Given  $v_0 \in \mathbb{S}$ , for any  $k \leq O(1/\eta)$ , we have*

$$\|v_k\|^2 \leq 1 + O\left(\frac{\eta}{(1-\mu)^3}\right).$$

Moreover, there exists a constant  $C > 0$ , which does not depend on the step size  $\eta$  and  $\mu$ , such that

$$\|v_{k+1} - v_k\| \leq \frac{C\eta}{1-\mu}, \quad (3.1)$$

where  $C = \sup_{\|v\| \leq 2, \|X\| \leq C_d} \|XX^T v - v^T XX^T v v\|$ .

Combining Lemma 3.2 and Theorem A.5, tightness can be proved. Then by Prokhorov's Theorem, we know for any subsequence of  $\{V^\eta(\cdot)\}_\eta$ , there is a further subsequence that converges weakly. Furthermore, since the discontinuity goes to zero, the weak-sense limit must be continuous.

We next compute the weak limit. For simplicity, we define

$$\beta_k = \sum_{i=0}^{k-1} \mu^{k-i} \left[ (\Sigma_i - \Sigma)v_i - v_i^T (\Sigma_i - \Sigma)v_i v_i \right] \quad \text{and} \quad \epsilon_k = (\Sigma_k - \Sigma)v_k - v_k^T (\Sigma_k - \Sigma)v_k v_k.$$

We then rewrite the algorithm as follows:

$$m_{k+1} = m_k + (1-\mu)[-m_k + \tilde{M}(v_k)], \quad (3.2)$$

$$v_{k+1} = v_k + \eta Z_k = v_k + \eta(m_{k+1} + \beta_k + \epsilon_k), \quad (3.3)$$

where  $\tilde{M}(v) = \frac{1}{1-\mu}[\Sigma v - v^T \Sigma v v]$ . Note here, if we know  $v_k$  and  $m_k$  exactly,  $m_{k+1}$  will be updated without any error. The basic idea of the proof is to view (3.2) and (3.3) as a two-time-scale algorithm, where  $m_k$  is updated with a larger step size  $(1-\mu)$  and thus under a faster time-scale, and  $v_k$  is under a slower one. Then we can treat the slower time-scale iterate  $v$  as static and replace the faster time-scale iterate  $m$  by its stable point in term of this fixed  $v$  in (3.3). This stable point is  $\tilde{M}(v)$ , and we have the following lemma.

**Lemma 3.3.** *For any  $k > 0$ ,*

$$\|m_{k+1}^\eta - \tilde{M}(v_k^\eta)\| \leq O(\eta \log(1/\eta)), \quad w.p.1.$$

Here, we highlight the dependence on the step size  $\eta$  by adding a superscript to  $m_k$ ,  $v_k$ , and other sequences we will use later. Following this lemma, we can replace  $m_{k+1}$  by  $\tilde{M}(v_k)$  in the slower iterations:

$$v_{k+1}^\eta = v_k^\eta + \eta[\tilde{M}(v_k^\eta) + [m_{k+1}^\eta - \tilde{M}(v_k^\eta)] + \beta_k^\eta + \epsilon_k^\eta]. \quad (3.4)$$

Then, we have the main theorem of this section.

**Theorem 3.4.** *Suppose  $v_0 = v_1 \in \mathbb{S}$ . Then for each subsequence of  $\{V^\eta(\cdot), \eta > 0\}$ , there exists a further subsequence and a process  $V(\cdot)$  such that*

$$V^\eta(\cdot) \Rightarrow V(\cdot)$$

*in the weak sense as  $\eta \rightarrow 0$  through the convergent subsequence, where  $V(\cdot)$  satisfies the following ODE:*

$$\dot{V} = \frac{1}{1-\mu}[\Sigma V - V^T \Sigma V V], \quad V(0) = v_0. \quad (3.5)$$

To prove this theorem, we show that the continuous time interpolation of the error

$$[m_{k+1}^\eta - \tilde{M}(v_k^\eta)] + \beta_k^\eta + \epsilon_k^\eta$$

converges weakly to a Lipschitz continuous martingale with zero initialization. From the martingale theory, we know such kind of martingales must be a constant. Thus, the error sequence converges weakly to zero, and what is left in (3.4) is clearly the discretization of ODE (3.5). Please refer to Appendix B.3 for detailed proof.

To solve ODE (3.5), we need to rotate the coordinate to decouple each dimension. Under Assumption 1, there exists an orthogonal matrix  $Q$  such that:

$$\Sigma = Q \Lambda Q^T,$$

where  $\Lambda = \text{diag}(\lambda_1, \lambda_2, \dots, \lambda_d)$ . Let  $h_k = Q^T v_k$  and  $Y_k = Q^T X_k$ . Multiply each side of (2.3) by  $Q^T$ , and we get

$$h_{k+1} = h_k + \mu(h_k - h_{k-1}) + \eta[\Lambda_k h_k - h_k^T \Lambda_k h_k h_k], \quad (3.6)$$

where  $\Lambda_k = Y_k Y_k^T$ .

**Remark 3.5.** The landscape after this linear transformation is clear. Define the manifold gradient operator as

$$GD(H) = \Lambda H - H^T \Lambda H H.$$

Then for  $1 \leq i \leq d$ ,  $GD(e_i) = 0$ , which implies  $e_i, i \geq 1$  are all the non-zero stationary points up to sign change. The Jacobian Matrix of  $GD$  at  $e_i$  is defined as  $A_i$ , where

$$A_i = \text{diag}\{\lambda_1 - \lambda_i, \dots, -2\lambda_i, \dots, \lambda_d - \lambda_i\},$$

where  $-2\lambda_i$  is the  $i$ -th diagonal entry. Note here, under Assumption 1, only  $A_1$  is negative definite, while  $A_i, i \geq 2$  all have positive eigenvalues. Thus,  $H^* = e_1$  is the only global optimum up to sign change. Without loss of generality, we only consider  $e_1$  throughout the rest of the paper.

The continuous interpolation of  $\{h_k^\eta\}_{k=1}^\infty$  is  $H^\eta(t) = Q^T V^\eta(t)$ . Then, we rewrite ODE (3.5) as:

$$\dot{H} = \frac{1}{1-\mu} [\Lambda H - H^T \Lambda H H]. \quad (3.7)$$

Here, let  $M(H) \triangleq \frac{1}{1-\mu} [\Lambda H - H^T \Lambda H H]$  for simplicity. The ODE (3.7) is different from that in (4.6) in Chen et al. (2017) by a constant  $\frac{1}{1-\mu}$ . Then we have the following corollary.

**Corollary 3.6.** Suppose  $H^\eta(0) = H(0) \in \mathcal{S}$ . As  $\eta \rightarrow 0$ ,  $\{H^\eta(\cdot), \eta > 0\}$  converges weakly to

$$H^{(i)}(t) = C(t)^{-\frac{1}{2}} H^{(i)}(0) \exp\left(\frac{\lambda_i t}{1-\mu}\right), i = 1, \dots, d,$$

where  $C(t) = \sum_{i=1}^d [H^{(i)}(0) \exp(\frac{\lambda_i t}{1-\mu})]^2$ . Moreover, given  $H^{(1)}(0) \neq 0$ ,  $H(t)$  converges to  $H^* = e_1$  as  $t \rightarrow \infty$ .

Corollary 3.6 implies that when not initialized at saddle points or minima, the algorithm asymptotically converges to the global optimum. However, such a deterministic ODE-based approach is insufficient to characterize the local algorithmic behavior, since the noise of the stochastic gradient diminishes as  $\eta \rightarrow 0$ . Thus, we resort to the following SDE-based approach for a more precise characterization.

## 4 Analyzing Local Dynamics by SDE

To characterize the local algorithmic behavior, we need to rescale the influence of the noise. For this purpose, we consider the *normalized error*  $\frac{h_k - e_i}{\sqrt{\eta}}$  under the diffusion approximation framework. Different from the previous ODE-based approach, we obtain an SDE approximation here. Intuitively, the previous ODE-based approach is analogous to the Law of Large Number for random variables, while the SDE-based approach serves the same role as Central Limit Theorem. For consistency, we first study the algorithmic behavior around the global optimum.

#### 4.1 Phase III: Around Global Optima ( $\mathcal{R}_3$ )

Recall that all the coordinates are decoupled after the rotation. We directly consider each individual coordinate separately. For the  $i$ -th coordinate,  $i \neq 1$ , we define the normalized process  $u_k^{\eta,i} = h_k^{\eta,i} / \sqrt{\eta}$ , where  $h_k^{\eta,i}$  is the  $i$ -th dimension of  $h_k^\eta$ . Accordingly,  $U^{\eta,i}(t) = H^{\eta,i}(t) / \sqrt{\eta}$ . The next theorem characterizes the limiting process of  $U^{\eta,i}(t)$ .

**Theorem 4.1.** *As  $\eta \rightarrow 0$ ,  $\{U^{\eta,i}(\cdot)\}$  ( $i \neq 1$ ) converges weakly to a stationary solution of*

$$dU = \frac{(\lambda_i - \lambda_1)}{1 - \mu} U dt + \frac{\alpha_{i,1}}{(1 - \mu)} dB_t, \quad (4.1)$$

where  $\alpha_{i,j} = \sqrt{\mathbb{E}[(Y^{(i)})^2(Y^{(j)})^2]} < \infty$  by Assumption 2.

Note that our analysis is very different from that in [Chen et al. \(2017\)](#) because of the failure of IPA due to the similar blow-up issue. We remark that our technique mainly relies on Theorem A.6 (in Appendix A) from [Kushner and Yin \(2003\)](#). Since the proof is much more sophisticated and involved than IPA, we only introduce the key technique, Fixed-State-Chain, in a high level.

*Proof Sketch.* Note that the algorithm can be rewritten as

$$\begin{aligned} h_{k+1}^{\eta,i} &= h_k^{\eta,i} + \eta \left[ \sum_{j=1}^{k-1} \mu^{k-j} (\Lambda_j h_j^\eta - (h_j^\eta)^T \Lambda_j h_j^\eta h_j^\eta) \right. \\ &\quad \left. + \Lambda h_k^\eta - (h_k^\eta)^T \Lambda h_k^\eta h_k^\eta \right]^{(i)} \\ &\quad + \eta \left[ (\Lambda_k - \Lambda) h_k^\eta - (h_k^\eta)^T (\Lambda_k - \Lambda) h_k^\eta h_k^\eta \right]^{(i)}. \end{aligned}$$

Here, for a vector  $x \in \mathbb{R}^d$  and an integer  $i \leq d$ ,  $x^{(i)}$  represents the  $i$ -th dimension of  $x$ . In particular, we define

$$\begin{aligned} \xi_k^{(i)} &= \left[ \sum_{j=1}^{k-1} \mu^{k-j} (\Lambda_j h_j - h_j^T \Lambda_j h_j h_j) + \Lambda h_k - h_k^T \Lambda h_k h_k \right]^{(i)}, \\ \gamma_k^{(i)} &= [(\Lambda_k - \Lambda) h_k - h_k^T (\Lambda_k - \Lambda) h_k h_k]^{(i)}, \\ g^{(i)}(\xi_k, h_k) &= \xi_k^{(i)} + [\Lambda h_k - h_k^T \Lambda h_k h_k]^{(i)}, \\ Z_k^{(i)} &= g^{(i)}(\xi_k, h_k) + \gamma_k^{(i)}. \end{aligned}$$

Here,  $g$  is the accelerated gradient flow, and  $\gamma_k$  is the noise. Then the algorithm becomes

$$h_{k+1}^{\eta,i} = h_k^{\eta,i} + \eta Z_k^{\eta,i} = h_k^{\eta,i} + \eta g^{(i)}(\xi_k^\eta, h_k^\eta) + \eta \gamma_k^{\eta,i},$$

and thus we have

$$u_{k+1}^{\eta,i} = u_k^{\eta,i} + \sqrt{\eta} [g^{(i)}(\xi_k^\eta, h_k^\eta) + \gamma_k^{\eta,i}].$$

Note here

$$g(\xi_k^\eta, h_k^\eta) \in \mathcal{F}_k^\eta \quad \text{and} \quad \mathbb{E}[\gamma_k^{\eta,i} | \mathcal{F}_k^\eta] = 0,$$

which implies the noise is a martingale difference sequence.

We then manipulate the algorithm to extract the Markov structure of the algorithm in an explicit form. To make it clear, given  $H$ , there exists a transition function  $P(\cdot, \cdot | H)$  such that

$$P\{\xi_{k+1}^{\eta,i} \in \cdot | \mathcal{F}_k^\eta\} = P(\xi_k^{\eta,i}, \cdot | H = h_k^{\eta,i}).$$

This comes from the observation that

$$\xi_{k+1}^{(i)} = \mu \xi_k^{(i)} + \mu(\Lambda_k h_k - h_k^T \Lambda_k h_k h_k)^{(i)},$$

where the randomness only comes from the data when the state  $h_k$  is given. Then the fixed-state-chain refers to the Markov chain with transition function  $P(\cdot, \cdot | H)$  for a fixed  $H$ . The state of this Markov chain will be denoted by  $\{\xi_k(H)\}$ . We then decompose  $h_{k+1}^{\eta,i} - h_k^{\eta,i}$  into three parts

$$\begin{aligned} h_{k+1}^{\eta,i} - h_k^{\eta,i} &= \eta g^{(i)}(\xi_k(h_k^\eta), h_k^\eta) + \eta[g^{(i)}(\xi_k^\eta, h_k^\eta) - g^{(i)}(\xi_k(h_k^\eta), h_k^\eta)] + \eta \gamma_k^{\eta,i} \\ &= \eta M^{(i)}(h_k^\eta) + \eta \gamma_k^{\eta,i} + \eta[g^{(i)}(\xi_k(h_k^\eta), h_k^\eta) - M^{(i)}(h_k^\eta)] + \eta[g^{(i)}(\xi_k^\eta, h_k^\eta) - g^{(i)}(\xi_k(h_k^\eta), h_k^\eta)] \\ &= \eta M^{(i)}(h_k^\eta) + \eta W_k^{\eta,i}. \end{aligned} \tag{4.2}$$

Here,  $W_k^{\eta,i}$  is the error term. By (4.2), we find that the error comes from three sources:

- Difference between the fixed-state-chain and the limiting process:  $g^{(i)}(\xi_k(h_k), h_k) - M^{(i)}(h_k)$ ;
- Difference between the accelerated gradient flow and the fixed-state-chain:  $g^{(i)}(\xi_k, h_k) - g^{(i)}(\xi_k(h_k), h_k)$ ;
- The noise  $\gamma_k^{(i)}$ .

We then handle them separately and combine the results together to get the variance of  $W_k^{\eta,i}$ . Then  $\{u_k^{\eta,i}\}$  follows:

$$u_{k+1}^{\eta,i} - u_k^{\eta,i} = \eta \frac{M^{(i)}(h_k^\eta)}{\sqrt{\eta}} + \sqrt{\eta} W_k^{\eta,i}.$$

Together with the fact that around  $H^*$ ,

$$M^{(i)}(h) = \frac{(\lambda_i - \lambda_1)}{1 - \mu} h^{(i)} + o(|h^{(i)}|),$$

we further know

$$\frac{u_{k+1}^{\eta,i} - u_k^{\eta,i}}{\eta} \approx \frac{(\lambda_i - \lambda_1)}{1 - \mu} u_k^{\eta,i} + \frac{W_k^{\eta,i}}{\sqrt{\eta}}. \tag{4.3}$$

After calculating the variance of  $W$ , we see that (4.3) is essentially the discretization of SDE (4.1). For detailed proof, please refer to Appendix C.1.  $\square$

Differential equation (4.1) admits an explicit solution which is known as an O-U process Øksendal (2003) defined as:

$$U^{(i)}(t) = \frac{\alpha_{i,1}}{1-\mu} \int_0^t \exp\left[\frac{\lambda_i - \lambda_1}{1-\mu}(s-t)\right] dB(s) + U^{(i)}(0) \exp\left[\frac{\lambda_i - \lambda_1}{1-\mu}t\right].$$

Its expectation and variance are:

$$\mathbb{E}[U^{(i)}(t)] = U^{(i)}(0) \exp\left[\frac{\lambda_i - \lambda_1}{1-\mu}t\right], \quad \text{Var}[U^{(i)}(t)] = \frac{1}{1-\mu} \frac{\alpha_{i,1}^2}{2(\lambda_1 - \lambda_i)} \left(1 - \exp\left[2\frac{\lambda_i - \lambda_1}{1-\mu}t\right]\right).$$

We see clearly that the momentum essentially increases the variance of the normalized error by a factor of  $\frac{1}{1-\mu}$  around the global optimum. Thus, it becomes harder for the algorithm to converge.

More precisely, given a pre-specified  $\epsilon > 0$ , the algorithm enters the  $\epsilon$ -neighborhood of the global optimum when

$$\sum_{i=2}^d \left(h_\eta^{(i)}(T_3)\right)^2 \leq \epsilon.$$

For notational simplicity, define  $\alpha^2 = \max_{1 \leq i \leq d} \alpha_{i,1}^2$ . We have the following lemma.

**Lemma 4.2.** *Given a pre-specified  $\epsilon > 0$ , to enter the  $\epsilon$ -neighborhood of the global optimum with probability at least  $\frac{3}{4}$  (or a constant probability) at some time  $T_3$ , the step size  $\eta$  must satisfy the following inequality:*

$$\eta < \frac{(1-\mu)(\lambda_1 - \lambda_2)\epsilon}{2d\alpha^2}. \quad (4.4)$$

Note that Chen et al. (2017) choose the step size of SGD as

$$\eta_0 \asymp \frac{(\lambda_1 - \lambda_2)\epsilon}{d\alpha^2}, \quad (4.5)$$

which does not satisfy (4.4) for  $\mu$  close to 1. Thus, if we use the same step size of SGD, MSGD cannot converge, since the variance increased by the momentum becomes too large. To handle this issue, we have to decrease the step size by a factor  $1 - \mu$ , i.e.

$$\eta \asymp (1-\mu) \frac{\epsilon(\lambda_1 - \lambda_2)}{d\alpha^2} \asymp (1-\mu)\eta_0. \quad (4.6)$$

Then we obtain the following proposition.

**Proposition 4.3.** *Given a pre-specified  $\epsilon > 0$  and  $\eta$  as defined in (4.6), there exists some constant  $\delta = O(\sqrt{\eta})$ , such that after restarting the counter of time, if  $\left(H_\eta^{(1)}(0)\right)^2 \geq 1 - \delta^2$ , we then need*

$$T_3 = \frac{(1-\mu)}{2(\lambda_1 - \lambda_2)} \log K_3,$$

where  $K_3 = \frac{(1-\mu)(\lambda_1 - \lambda_2)\delta^2}{(1-\mu)(\lambda_1 - \lambda_2)\epsilon - 2d\eta\alpha^2}$ , to ensure  $\sum_{i=2}^d \left(h_\eta^{(i)}(T_3)\right)^2 \leq \epsilon$  with probability at least  $3/4$ .

This implies that the algorithm needs at most

$$N_3 \approx \frac{T_3}{\eta} = \tilde{\mathcal{O}} \left[ \frac{d\alpha^2}{\epsilon(\lambda_1 - \lambda_2)^2} \right]$$

iterations to converge to an  $\epsilon$ -optimal solution in Phase III. Note that  $\tilde{\mathcal{O}}(\cdot)$  hides some log factors, which are not important. This result matches that for SGD. We remark here that this small step size (4.6) is *only* used for Phase III, but not for the other two phases.

## 4.2 Phase II: How MSGD Traverses between Stationary Points ( $\mathcal{R}_2$ )

For Phase II, we characterize how the algorithm behaves, once it has escaped from saddle points. During this period, MSGD is dominated by the gradient, and the influence of the noise is negligible. Thus, the algorithm experiences almost a deterministic traverse between stationary points, and we can use the ODE approximation to study its behavior before it enters the neighborhood of the optimum. By Corollary 3.6, we obtain the following proposition.

**Proposition 4.4.** *After restarting the counter of time, given  $\eta = \eta_0$  as defined in (4.5),  $\delta = \mathcal{O}(\sqrt{\eta_0})$ , we need*

$$T_2 = \frac{(1 - \mu)}{2(\lambda_1 - \lambda_2)} \log \left( \frac{1 - \delta^2}{\delta^2} \right)$$

such that  $\left( H_\eta^{(1)}(T_2) \right)^2 \geq 1 - \delta^2$ .

Note that in Proposition 4.4, we use  $\eta = \eta_0$ , which is the same as SGD (much larger than (4.6) for  $\mu$  close to 1). This result implies that the algorithm needs at most

$$N_2 \approx \frac{T_2}{\eta} = \tilde{\mathcal{O}} \left[ \frac{(1 - \mu)d\alpha^2}{\epsilon(\lambda_1 - \lambda_2)^2} \right]$$

iterations to traverse between stationary points. Clearly, MSGD is faster than SGD by a factor of  $1 - \mu$  in Phase II, when using the same step size. This is because the algorithm can make more progress along the descent direction with the help of the momentum.

## 4.3 Phase I: Escaping from Saddle Points ( $\mathcal{R}_1$ )

At last, we study the algorithmic behavior around saddle points  $e_j$ ,  $j \neq 1$ . By the same SDE approximation technique used in Section 4.1, we obtain the following theorem.

**Theorem 4.5.** *Condition on the event that  $h_k^n - e_j = \mathcal{O}(\sqrt{\eta})$  for  $k = 1, 2, \dots$ . Then for  $i \neq j$ ,  $\{U^{\eta,i}(\cdot)\}$  converges weakly to a solution of*

$$dU = \frac{(\lambda_i - \lambda_j)}{1 - \mu} U dt + \frac{\alpha_{i,j}}{(1 - \mu)} dB_t.$$

We remark that  $h_k^\eta - e_j = \mathcal{O}(\sqrt{\eta})$  is only a technical assumption. This does not cause any issue since when  $(h_k^\eta - e_j)/\sqrt{\eta}$  is large, or equivalently  $(H_\eta^{(j)}(T_1))^2$  is smaller than  $1 - \delta^2$  ( $\delta = \mathcal{O}(\sqrt{\eta})$ ), MSGD has escaped from the saddle point  $e_j$ , which is out of Phase I.

Theorem 4.5 implies that for  $i > j$ , the process defined by the equation above is an unstable O-U process, which goes to infinity. Thus, the algorithm will not be trapped around saddle points. Then we obtain the following proposition.

**Proposition 4.6.** *Given a pre-specified  $\nu \in (0, 1)$ ,  $\eta = \eta_0$  as defined in (4.5), and  $\delta = \mathcal{O}(\sqrt{\eta_0})$ , then the following result holds: We need*

$$T_1 = \frac{1 - \mu}{2(\lambda_1 - \lambda_2)} \log(2K_1 + 1), \quad (4.7)$$

where  $K_1 = \frac{(1 - \mu)\eta_0^{-1}\delta^2(\lambda_1 - \lambda_2)}{\Phi^{-1}\left(\frac{1+\nu}{2}\right)^2 \alpha_{12}^2}$ , such that  $(H_\eta^{(2)}(T_1))^2 \leq 1 - \delta^2$  with probability at least  $1 - \nu$ , where  $\Phi(x)$  is the CDF of the standard normal distribution.

Proposition 4.6 suggests that we need approximately

$$N_1 \approx \frac{T_1}{\eta} = \tilde{\mathcal{O}}\left[\frac{(1 - \mu)d\alpha^2}{\varepsilon(\lambda_1 - \lambda_2)^2}\right]$$

iterations to escape from saddle points. Thus, when using the same step size, MSGD can escape from saddle points in less iterations than SGD by a factor of  $1 - \mu$ . This is due to the fact that the momentum can greatly increase the variance and perturb the algorithm more violently. Thus, it becomes harder to stay around saddle points. Moreover, the momentum also encourages more aggressive exploitation, and in each iteration, the algorithm makes more progress along the descent direction by a factor of  $\frac{1}{1-\mu}$ .

## 5 Some Insights on Training DNNs

The streaming PCA problem is closely related to optimization for deep neural networks (DNNs) from many aspects. Existing literature has shown that the optimization landscape of training DNNs, though much more complicated and difficult to analyze, consists of similar basic geometric structures, such as saddle points and local optima. Thus, our theoretical characterization of the algorithmic behavior of MSGD around saddle points and local optima (for the streaming PCA problem) can provide us new insights of how MSGD behave in training DNNs.

Choromanska et al. (2015); Dauphin et al. (2014); Kawaguchi (2016); Hardt and Ma (2016) suggest that there are a combinatorially large number of saddle points and many local optima in training DNNs. Under certain *oversimplified* conditions, they prove: When the size of the network is large enough, most local optima are equivalent and yield similar generalization performance; Moreover, the probability of achieving a “spurious/bad” local optimum (which does not generalize well), though not zero, decreases exponential fast, as the size of the network gets larger. Thus,

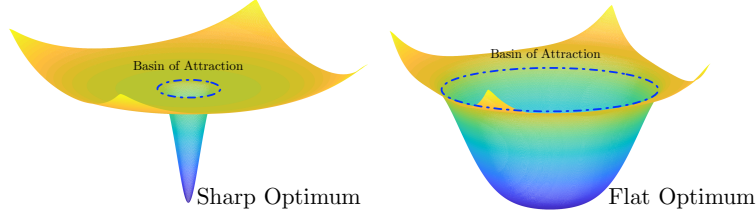


Figure 1: Two illustrative examples of the flat and sharp local optima. MSGD tends to avoid the sharp local optimum, since its high variance encourages exploration.

they suspect that the major computational challenge of training DNNs should be “how efficient an algorithm is when escaping from numerous saddle points.” From this aspect, our Proposition 4.6 suggests that *MSGD indeed escapes from saddle points faster than VSGD in existence of negative curvatures*.

“No spurious/bad local optima”, however, is often considered as an overoptimistic claim. Some recent results Hochreiter and Schmidhuber (1997); Keskar et al. (2016); Zhang et al. (2017); Neyshabur et al. (2017); Safran and Shamir (2017) provide some empirical and theoretical evidences that the spurious/bad local optima are not completely negligible. Keskar et al. (2016); Zhang et al. (2017); Neyshabur et al. (2017) further suggest that the landscape of these spurious/bad local optima is usually sharp, i.e., their basin of attractions are small and wiggle (as illustrated in Figure 1). From this aspect, our Lemma 4.2 suggests that MSGD with a larger momentum ( $\mu$  is very close to 1) tends to stay in “flat/good local optima”, since the higher variance of the noise introduced by the momentum encourages more exploration outside the small basin of attraction of sharp local optima.

Our analysis also provides some new insights on how to apply the step size annealing technique to MSGD. Specifically, our Lemma 4.2 suggests that at the final stage of the step size annealing, MSGD should use a much smaller step size than that of VSGD. Otherwise, MSGD may be numerically unstable and fails to converge well.

## 6 Numerical Experiments

We present numerical experiments for both streaming PCA and training deep neural networks. The experiments on streaming PCA verify our theory in Section 4, and the experiments on training deep neural networks verify some of our discussions in Section 5.

### 6.1 Streaming PCA

We first provide a numerical experiment to verify our theory for streaming PCA. We set  $d = 4$  and the covariance matrix  $\Lambda = \text{diag}\{4, 3, 2, 1\}$ . The optimum is  $(1, 0, 0, 0)$ . Figure 2 compares the performance of VSGD, MSGD (with and without the step size annealing in Phase III). The initial solution is the saddle point  $(0, 1, 0, 0)$ . We choose  $\mu = 0.9$  and  $\eta = 5 \times 10^{-4}$ , and decrease the step

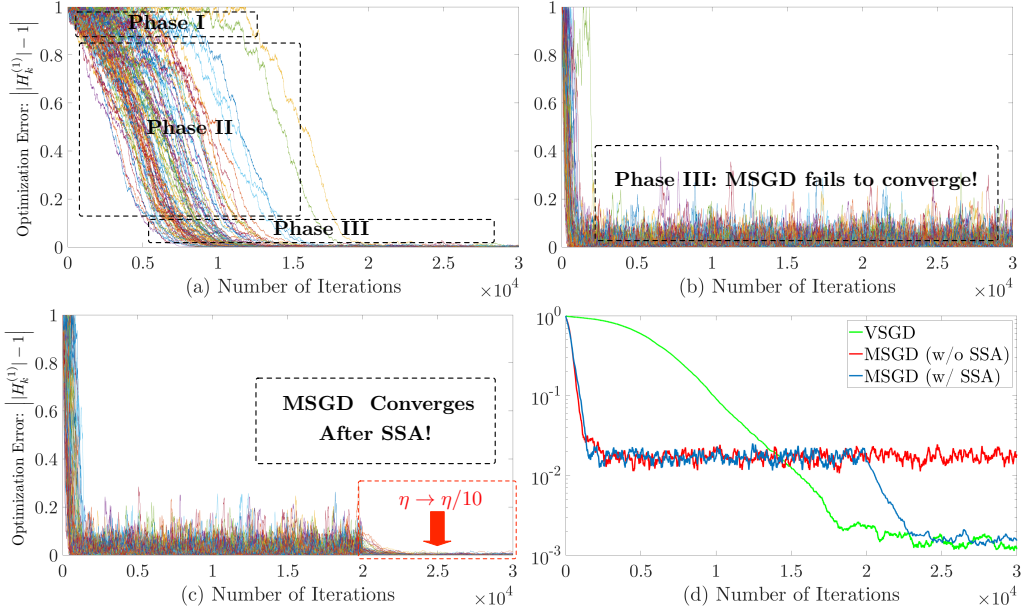


Figure 2: Comparison between SGD and MSGD (with and without the step size annealing (SSA) in Phase III).

size of MSGD by a factor  $1 - \mu$  after  $2 \times 10^4$  iterations in Fig.2.c. Fig.2.a-c plot the results of 100 simulations, and the vertical axis corresponds to  $||H_k^{(1)} - 1|$ . We can clearly differentiate the three phases of VSGD in Fig.2.a. For MSGD in Fig.2.b, we hardly recognize Phases I and II, since they last for a much shorter time. This is because the momentum significantly helps escape from saddle points and evolve toward global optima. Moreover, we also observe that MSGD without the step size annealing does not converge well, but the step size annealing resolves this issue. All these observations are consistent with our analysis. Fig.2.d plots the optimization errors of these three algorithms averaged over all 100 simulations, and we observe similar results.

## 6.2 Deep Neural Networks

We then provide three experiments to compare MSGD with VSGD in training a ResNet-18 DNN using the CIFAR-100 dataset for a 100-class image classification task. We choose a batch size of 128. 50k images are used for training, and the rest 10k are used for testing. We repeat each experiment for 10 times and report the average.

$$\tilde{\eta}_M \in \{0.5, 0.2, 0.1, 0.05, 0.02, 0.01\} \quad \text{and} \quad \tilde{\eta}_V \in \{1, 0.5, 0.2, 0.1, 0.05, 0.02, 0.01\}$$

denote the initial step sizes of MSGD and VSGD, respectively. We decrease the step size by a factor of 0.1 after 87, 128, and 160 epochs. More details on the network architecture and experimental settings can be found in Appendix D. We plot the obtained results in Figure 5

- **Experiment 1.** The results are shown in Fig.5. Choosing  $\tilde{\eta}_M = \tilde{\eta}_V$ ,  $\mu = 0.9$ , MSGD achieves better generalization than VSGD.

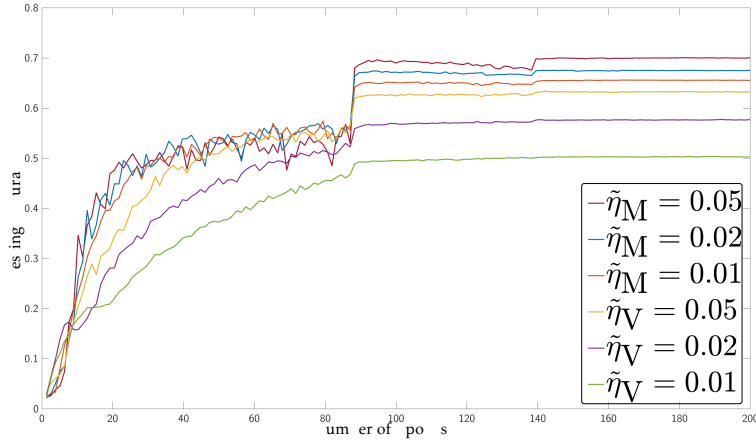


Figure 3: Experimental results on CIFAR-100 for training DNNs. MSGD and VSGD are using the same step sizes.

- **Experiment 2.** The results are shown in Fig.5. Choosing  $\frac{\tilde{\eta}_M}{1-\mu} = \tilde{\eta}_V$ ,  $\mu = 0.9$ , MSGD achieves similar generalization to VSGD (when  $\frac{\tilde{\eta}_M}{1-\mu} \leq 0.5$ ).

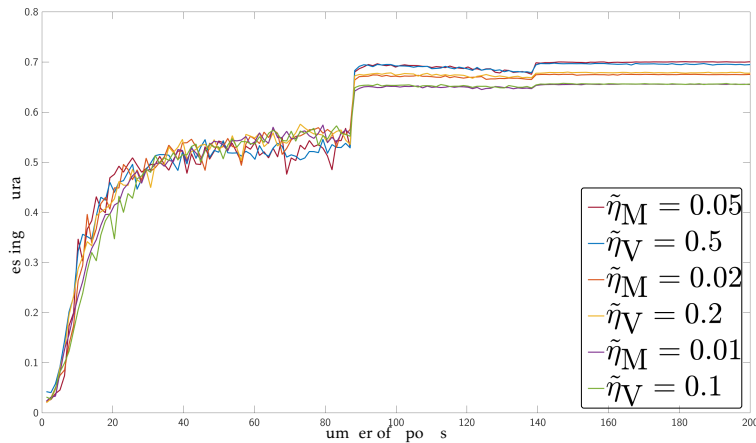


Figure 4: Experimental results on CIFAR-100 for training DNNs. VSGD is using the step sizes of MSGD rescaled by  $1/(1-\mu)$ .

- **Experiment 3.** The results are shown in Fig.5. For MSGD, choosing  $\mu = 0.9$  and  $\tilde{\eta}_M = 0.2$  achieves the optimal generalization (among all possible values). For VSGD, choosing  $\tilde{\eta}_M = 0.5$  achieves the optimal generalization (among all possible values). We see that the optimal generalization of MSGD is better than that of VSGD. Note that for  $\frac{\tilde{\eta}_M}{1-\mu} = 1$  and 2, MSGD still works well. However, for  $\tilde{\eta}_V = 1$ , VSGD no longer works, and the generalization drops significantly.

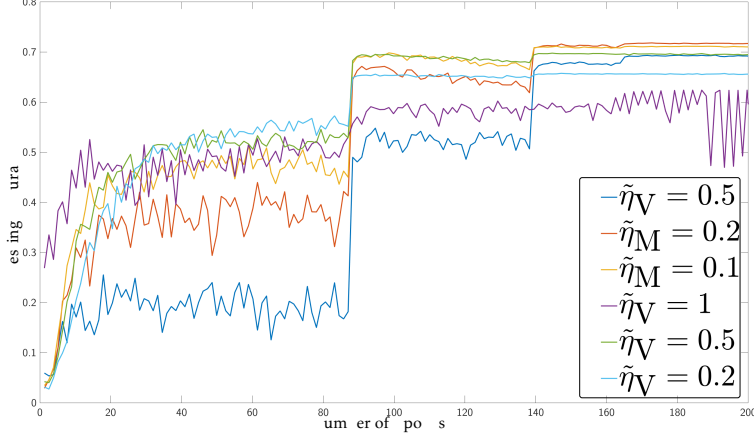


Figure 5: *Experimental results on CIFAR-100 for training DNNs. MSGD and VSGD are using their optimal step sizes.*

## 7 Discussions

The results on training DNNs are expectable or partially expectable, given our theoretical analysis for streaming PCA. We remark that our experiments (in Fig.5 Bottom) show some inconsistency with an earlier paper [Wilson et al. \(2017\)](#). Specifically, [Wilson et al. \(2017\)](#) show that MSGD does not outperform VSGD in training a VGG-16 deep neural network using the CIFAR-10 dataset. However, our results show that the momentum indeed improves the training. We suspect that there exist certain structures in the optimization landscape of VGG-16, which marginalize the value of MSGD. In contrast, the optimization landscape of ResNet-18 is more friendly to MSGD than VGG-16.

Moreover, we remark that our theory helps explain some phenomena in training DNNs, however, there still exist some gaps: (1) Our analysis requires  $\eta \rightarrow 0$  to do the diffusion approximation. However, the experiments actually use relatively large step sizes at the early stage of training. Though we can expect large and small step sizes share some similar behaviors, it may lead to very different results. For example, we observe that VSGD can use larger step sizes, and achieve similar generalization to that of MSGD. However, when MSGD achieves the optimal generalization using  $\frac{\tilde{\eta}_M}{1-\mu} = 2$ , VSGD performs much worse using  $\tilde{\eta}_V = 2$ ; (2) The optimization landscape of DNNs also contains a vast amount of *high order saddle points*, where our analysis cannot be applied (neither all existing analyses). How SGD/MSGD behaves in this scenario is still an open theoretical problem.

## References

BONNABEL, S. (2013). Stochastic gradient descent on riemannian manifolds. *IEEE Transactions on Automatic Control* **58** 2217–2229.

- CHEN, Z., YANG, F. L., LI, C. J. and ZHAO, T. (2017). Online multiview representation learning: Dropping convexity for better efficiency. *arXiv preprint arXiv:1702.08134* .
- CHOROMANSKA, A., HENAFF, M., MATHIEU, M., AROUS, G. B. and LECUN, Y. (2015). The loss surfaces of multilayer networks. In *Artificial Intelligence and Statistics*.
- DAUPHIN, Y. N., PASCANU, R., GULCEHRE, C., CHO, K., GANGULI, S. and BENGIO, Y. (2014). Identifying and attacking the saddle point problem in high-dimensional non-convex optimization. In *Advances in neural information processing systems*.
- GHADIMI, S. and LAN, G. (2016). Accelerated gradient methods for nonconvex nonlinear and stochastic programming. *Mathematical Programming* **156** 59–99.
- HARDT, M. and MA, T. (2016). Identity matters in deep learning. *arXiv preprint arXiv:1611.04231* .
- HOCHREITER, S. and SCHMIDHUBER, J. (1997). Flat minima. *Neural Computation* **9** 1–42.
- KAWAGUCHI, K. (2016). Deep learning without poor local minima. In *Advances in Neural Information Processing Systems*.
- KESKAR, N. S., MUDIGERE, D., NOCEDAL, J., SMELYANSKIY, M. and TANG, P. T. P. (2016). On large-batch training for deep learning: Generalization gap and sharp minima. *arXiv preprint arXiv:1609.04836* .
- KRASULINA, T. (1970). Method of stochastic approximation in the determination of the largest eigenvalue of the mathematical expectation of random matrices. *Automation and Remote Control* 50–56.
- KRICHENE, W. and BARTLETT, P. L. (2017). Acceleration and averaging in stochastic mirror descent dynamics. *arXiv preprint arXiv:1707.06219* .
- KUSHNER, H. J. and YIN, G. G. (2003). Stochastic approximation and recursive algorithms and applications, stochastic modelling and applied probability, vol. 35.
- LI, C. J., WANG, Z. and LIU, H. (2016). Online ica: Understanding global dynamics of nonconvex optimization via diffusion processes. In *Advances in Neural Information Processing Systems*.
- LI, Q., TAI, C. and WEINAN, E. (2017). Stochastic modified equations and adaptive stochastic gradient algorithms. In *International Conference on Machine Learning*.
- LIU, W., ZHANG, Y.-M., LI, X., YU, Z., DAI, B., ZHAO, T. and SONG, L. (2017). Deep hyperspherical learning. In *Advances in Neural Information Processing Systems*.
- NEYSHABUR, B., BHOJANAPALLI, S., MCALLESTER, D. and SREBRO, N. (2017). Exploring generalization in deep learning. In *Advances in Neural Information Processing Systems*.

- OJA, E. (1992). Principal components, minor components, and linear neural networks. *Neural networks* **5** 927–935.
- OJA, E. and KARHUNEN, J. (1985). On stochastic approximation of the eigenvectors and eigenvalues of the expectation of a random matrix. *Journal of mathematical analysis and applications* **106** 69–84.
- ØKSENDAL, B. (2003). Stochastic differential equations. In *Stochastic differential equations*. Springer, 65–84.
- PANAGEAS, I. and PILIOURAS, G. (2016). Gradient descent converges to minimizers: The case of non-isolated critical points. *CoRR, abs/1605.00405* .
- SAFRAN, I. and SHAMIR, O. (2017). Spurious local minima are common in two-layer relu neural networks. *arXiv preprint arXiv:1712.08968* .
- SAGITOV, S. (2013). Weak convergence of probability measures .
- SANGER, T. D. (1989). Optimal unsupervised learning in a single-layer linear feedforward neural network. *Neural networks* **2** 459–473.
- WANG, Y. (2017). Asymptotic analysis via stochastic differential equations of gradient descent algorithms in statistical and computational paradigms. *arXiv preprint arXiv:1711.09514* .
- WILSON, A. C., ROELOFS, R., STERN, M., SREBRO, N. and RECHT, B. (2017). The marginal value of adaptive gradient methods in machine learning. *arXiv preprint arXiv:1705.08292* .
- ZHANG, C., LIAO, Q., RAKHLIN, A., SRIDHARAN, K., MIRANDA, B., GOLOWICH, N. and POGGIO, T. (2017). Theory of deep learning iii: Generalization properties of sgd. Tech. rep., Center for Brains, Minds and Machines (CBMM).

## A Summary on Weak Convergence and Main Theorems

Here, we summarize the theory of weak convergence and theorems used in this paper. Recall that the continuous-time interpolation of the solution trajectory  $V^\eta(\cdot)$  is defined as  $V^\eta(t) = v_k^\eta$  on the time interval  $[k\eta, (k+1)\eta)$ . It has sample paths in the space of Càdlàg functions (right continuous and have left-hand limits) defined on  $\mathbb{R}^d$ , or *Skorokhod Space*, denoted by  $D^d[0, \infty)$ . Thus, the weak convergence we consider here is defined in this space  $D^d[0, \infty)$  instead of  $\mathbb{R}^d$ . The special metric  $\sigma$  in  $D^d[0, \infty)$  is called Skorokhod metric, and the topology generated by this metric is Skorokhod topology. Please refer to [Sagitov \(2013\)](#); [Kushner and Yin \(2003\)](#) for detailed explanations. The weak convergence in  $D^d$  is defined as follows:

**Definition A.1** (Weak Convergence in  $D^d[0, \infty)$ ). *Let  $\mathcal{B}$  be the minimal  $\sigma$ -field induced by Skorokhod topology. Let  $\{X_n, n < \infty\}$  and  $X$  be random variables on  $D^d[0, \infty)$  defined on a probability space  $(\Omega, P, \mathcal{F})$ . Suppose that  $P_n$  and  $P_X$  are the probability measures on  $(D^d, \mathcal{B})$  generated by  $X_n$  and  $X$ . We say  $P_n$  converges weakly to  $P$  ( $P_n \Rightarrow P$ ), if for all bounded and continuous real-valued functions  $F$  on  $D^d$ , the following condition holds:*

$$\mathbb{E}F(X_n) = \int F(x)dP_n(x) \rightarrow \mathbb{E}F(X) = \int F(x)dP(x) \quad (\text{A.1})$$

With an abuse of terminology, we say  $X_n$  converges weakly to  $X$  and write  $X_n \Rightarrow X$ .

Another important definition we need is *tightness*:

**Definition A.2.** *A set of  $D^d$ -valued random variables  $\{X_n\}$  is said to be tight if for each  $\delta > 0$ , there is a compact set  $B_\delta \in D^d$  such that:*

$$\sup_n P\{X_n \notin B_\delta\} \leq \delta. \quad (\text{A.2})$$

We care about tightness because it provides us a powerful way to prove weak convergence based on the following two theorems:

**Theorem A.3** (Prokhorov's Theorem). *Under Skorokhod topology,  $\{X_n(\cdot)\}$  is tight in  $D^d[0, \infty)$  if and only if it is relative compact which means each subsequence contains a further subsequence that converges weakly.*

**Theorem A.4** ([Sagitov \(2013\)](#), Theorem 3.8). *A necessary and sufficient condition for  $P_n \Rightarrow P$  is each subsequence  $P_{n'}$  contains a further subsequence  $P_{n''}$  converging weakly to  $P$ .*

Thus, if we can prove  $\{X_n(\cdot)\}$  is tight and all the further subsequences share the same weak limit  $X$ , then we have  $X_n$  converges weakly to  $X$ . However, (A.2) is hard to verified. We usually check another easier criteria. Let  $\mathcal{F}_t^n$  be the  $\sigma$ -algebra generated by  $\{X_n(s), s \leq t\}$ , and  $\tau$  denotes a  $\mathcal{F}_t^n$ -stopping time.

**Theorem A.5** ([Kushner and Yin \(2003\)](#), Theorem 3.3, Chapter 7). *Let  $\{X_n(\cdot)\}$  be a sequence of processes that have paths in  $D^d[0, \infty)$ . Suppose that for each  $\delta > 0$  and each  $t$  in a dense set in  $[0, \infty)$ , there is a compact set  $K_{\delta,t}$  in  $\mathbb{R}$  such that*

$$\inf_n P\{X_n(t) \in K_{\delta,t}\} \geq 1 - \delta, \quad (\text{A.3})$$

and for each positive  $T$ ,

$$\lim_{\delta} \limsup_n \sup_{|\tau| \leq T} \sup_{s \leq \delta} \mathbb{E} \min[\|X_n(\tau + s) - X_n(\tau)\|, 1] = 0. \quad (\text{A.4})$$

Then  $\{X_n(\cdot)\}$  is tight in  $D^d[0, \infty)$ .

This theorem is used in Section 3 to prove tightness of the trajectory of Momentum SGD.

At last, we provide the theorem we use to prove the SDE approximation. Let's consider the following algorithm:

$$\theta_{n+1}^\eta = \theta_n^\eta + \eta Y_n^\eta, \quad (\text{A.5})$$

where  $Y_n^\eta = g_n^\eta(\theta_n^\eta, \xi_n^\eta) + M_n^\eta$ , and  $M_n^\eta$  is a martingale difference sequence. Then the normalized process  $U_n^\eta = (\theta_n^\eta - \bar{\theta})/\sqrt{\epsilon}$  satisfies:

$$U_{n+1}^\eta = U_n^\eta + \sqrt{\eta} (g_n^\eta(\theta_n^\eta, \xi_n^\eta) + M_n^\eta). \quad (\text{A.6})$$

We further assume the fixed-state-chain exists as in Section 4.1 and use the same notation  $\xi_i(\theta)$  to denote the fixed- $\theta$ -process. Then we have the following theorem:

**Theorem A.6** (Kushner and Yin (2003), Theorem 8.1, Chapter 10). *Assume the following conditions hold:*

A.1 For small  $\rho > 0$ ,  $\{\|Y_n^\eta\|^2 I_{|\theta_n^\eta - \bar{\theta}| \leq \rho}\}$  is uniformly integrable.

A.2 There is a continuous function  $\bar{g}(\cdot)$  such that for any sequence of integers  $n_\eta \rightarrow \infty$  satisfying  $n_\eta \eta \rightarrow 0$  as  $\eta \rightarrow 0$  and each compact set  $A$ ,

$$\frac{1}{n_\eta} \sum_{i=jn_\eta}^{jn_\eta+n_\eta-1} E_{jn_\eta}^\eta [g_i^\eta(\theta, \xi_i(\theta)) - \bar{g}(\theta)] I_{\{\xi_{jn_\eta}^\eta\}} \rightarrow 0$$

in the mean for each  $\theta$ , as  $j \rightarrow \infty$  and  $\eta \rightarrow 0$ .

A.3 Define

$$\Gamma_n^\eta(\theta) = \sum_{i=n}^{\infty} (1-\eta)^{i-n} E_n^\eta [g_i^\eta(\theta, \xi_i(\theta)) - \bar{g}(\theta)],$$

where when  $E_n^\eta$  is used, the initial condition is  $\xi_n(\theta) = \xi_n^\eta$ . For the initial conditions  $\xi_n^\eta$  confined to any compact set,

$$\{\|\Gamma_n^\eta(\theta_n^\eta)\|^2 I_{|\theta_n^\eta - \bar{\theta}| \leq \rho}, \|\Gamma_n^\eta(\bar{\theta})\|^2; n, \eta\}$$

is uniformly integrable, and

$$E \left| E_n^\eta \Gamma_{n+1}^\eta(\theta_{n+1}^\eta) - \Gamma_{n+1}^\eta(\theta_n^\eta) \right|^2 I_{|\theta_n^\eta - \bar{\theta}| \leq \rho} = O(\eta^2).$$

A.4 There is a Hurwitz matrix  $A$  such that

$$\bar{g}(\theta) = A(\theta - \bar{\theta}) + o(\theta - \bar{\theta}).$$

A.5 There is a matrix  $\Sigma_0 = \{\sigma_{0,ij}; i, j = i, \dots, r\}$  such that as  $n, m \rightarrow \infty$ ,

$$\frac{1}{m} \sum_{i=n}^{n+m-1} E_n^\eta [M_i^\eta (M_i^\eta)' - \Sigma_0] I_{|\theta_n^\eta - \bar{\theta}| \leq \rho} \rightarrow 0$$

in probability.

A.6 There is a matrix  $\bar{\Sigma}_0 = \{\bar{\sigma}_{0,ij}; i, j = i, \dots, r\}$  such that as  $n, m \rightarrow \infty$ ,

$$\frac{1}{m} \sum_{i=n}^{n+m-1} E_n^\eta [g_i^\eta(\bar{\theta}, \xi_i(\bar{\theta})) (g_i^\eta(\bar{\theta}, \xi_i(\bar{\theta})))' - \bar{\Sigma}_0] \rightarrow 0$$

in probability.

A.7 Define another function

$$G_n^{\eta,i}(\theta, \xi_n^\eta) = E_n^\eta [\Gamma_{n+1}^\eta(\theta_n^\eta) [Y_n^\eta]' I_{|\theta_n^\eta - \bar{\theta}| \leq \rho} | \theta_n^\eta = \theta].$$

It needs to be a continuous function in  $(\theta, \xi_n^\eta)$ , uniformly in  $n$  and  $\eta$ .

A.8 There is a matrix  $\Sigma_1 = \{\sigma_{1,ij}; i, j = i, \dots, r\}$  such that as  $n, m \rightarrow \infty$ ,

$$\frac{1}{m} \sum_{i=n}^{n+m-1} E_n^\eta [G_n^{\eta,i}(\bar{\theta}, \xi_i(\bar{\theta})) - \Sigma_1] \rightarrow 0$$

in probability.

Then there exists a Wiener process  $W(\cdot)$  with covariance matrix  $\Sigma = \Sigma_0 + \bar{\Sigma}_0 + \Sigma_1 + \Sigma_1'$  such that  $\{U^\eta(\cdot)\}$  converges weakly to a stationary solution of

$$dU = AUdt + dW.$$

## B Detailed Proof in Section 3

### B.1 Proof of Lemma 3.2

*Proof.* First, if we assume  $\{v_k\}$  is uniformly bounded by 2, by formulation (3.6), we then have

$$\begin{aligned} v_{k+1} - v_k &= \mu(v_k - v_{k-1}) + \eta\{\Sigma_k v_k - v_k^T \Sigma_k v_k\}, \\ \implies v_{k+1} - v_k &= \sum_{i=0}^k \mu^{k-i} \eta\{\Sigma_i v_i - v_i^T \Sigma_i v_i\}, \\ \implies \|v_{k+1} - v_k\|_2 &\leq C_\delta \frac{\eta}{1 - \mu}, \end{aligned}$$

where  $C_\delta = \sup_{\|v\| \leq 2, \|X\| \leq C_d} \|XX^T v - v^T XX^T v v\|$ . Thus, the jump  $v_{k+1} - v_k$  is bounded. Next, we show the boundedness assumption on  $v$  can be taken off. In fact, with an initialization on  $\mathbb{S}$  (the sphere of the unit ball), the algorithm is bounded in a much smaller ball of radius  $1 + O(\eta)$ .

Recall  $\delta_{k+1} = v_{k+1} - v_k$ . Let's consider the difference between the norm of two iterates,

$$\begin{aligned}
\Delta_k &= \|v_{k+1}\|^2 - \|v_k\|^2 = \|\delta_{k+1}\|^2 + 2v_k^T \delta_{k+1} \\
\Delta_{k+1} - \Delta_k &= \|\delta_{k+2}\|^2 + 2v_{k+1}^T \delta_{k+2} - \|\delta_{k+1}\|^2 - 2v_k^T \delta_{k+1} \\
&= \|\delta_{k+2}\|^2 - \|\delta_{k+1}\|^2 + 2\mu v_{k+1}^T \delta_{k+1} + 2\eta v_{k+1}^T \Sigma_{k+1} v_{k+1} (1 - v_{k+1}^T v_{k+1}) - 2v_k^T \delta_{k+1} \\
&= \|\delta_{k+2}\|^2 - \|\delta_{k+1}\|^2 + 2\mu v_k^T \delta_{k+1} + 2\mu \|\delta_{k+1}\|^2 + 2\eta v_{k+1}^T \Sigma_{k+1} v_{k+1} (1 - v_{k+1}^T v_{k+1}) - 2v_k^T \delta_{k+1} \\
&= \|\delta_{k+2}\|^2 + \mu \|\delta_{k+1}\|^2 - (1 - \mu) (\|\delta_{k+1}\|^2 + 2v_k^T \delta_{k+1}) + 2\eta v_{k+1}^T \Sigma_{k+1} v_{k+1} (1 - v_{k+1}^T v_{k+1}) \\
&= \|\delta_{k+2}\|^2 + \mu \|\delta_{k+1}\|^2 - (1 - \mu) \Delta_k + 2\eta v_{k+1}^T \Sigma_{k+1} v_{k+1} (1 - v_{k+1}^T v_{k+1}) \\
&\leq \|\delta_{k+2}\|^2 + \mu \|\delta_{k+1}\|^2 - (1 - \mu) \Delta_k, \quad \text{when } \|v_{k+1}\| \geq 1.
\end{aligned}$$

Let  $\kappa = \inf\{i : \|v_{i+1}\| > 1\}$ , then

$$\Delta_{\kappa+1} \leq (1 + \mu) \left(\frac{C_\delta}{1 - \mu}\right)^2 \eta^2 + \mu \Delta_\kappa.$$

Moreover, if  $1 < \|v_{\kappa+i}\| \leq 2$  holds for  $i = 1, \dots, n < \frac{t}{\eta}$ , we have

$$\begin{aligned}
\Delta_{\kappa+i} &\leq (1 + \mu) \left(\frac{C_\delta}{1 - \mu}\right)^2 \eta^2 + \mu \Delta_{\kappa+i-1} \\
&\leq \frac{1 + \mu}{1 - \mu} \left(\frac{C_\delta}{1 - \mu}\right)^2 \eta^2 + \mu^i \Delta_\kappa.
\end{aligned}$$

Thus,

$$\begin{aligned}
\|v_{\kappa+n+1}\|^2 &= \|v_\kappa\|^2 + \sum_{i=0}^n \Delta_{\kappa+i} \\
&\leq 1 + \frac{1}{1 - \mu} \Delta_\kappa + \frac{t}{\eta} \frac{1 + \mu}{1 - \mu} \left(\frac{C_\delta}{1 - \mu}\right)^2 \eta^2 \\
&\leq 1 + O\left(\frac{\eta}{(1 - \mu)^3}\right).
\end{aligned}$$

In other words, when  $\eta$  is very small, we cannot go far from  $\mathbb{S}$  and the assumption that  $\|v\| \leq 2$  can be removed.  $\square$

## B.2 Proof of Lemma 3.3

*Proof.* Since  $\frac{1}{1-\mu} = \sum_{i=0}^{\infty} \mu^i$ , there exists  $N(\eta) = \log_{\mu}(1-\mu)\eta$  such that  $\sum_{i=N(\eta)}^{\infty} \mu^i < \eta$ . When  $k > N(\eta)$ , write  $m_k$  and  $\widetilde{M}(v_k)$  into summations:

$$\begin{aligned} m_{k+1} &= \sum_{i=0}^k \mu^i [\Sigma v_{k-i} - v_{k-i}^T \Sigma v_{k-i} v_{k-i}] \\ &= \sum_{i=0}^{N(\delta)} \mu^i [\Sigma v_{k-i} - v_{k-i}^T \Sigma v_{k-i} v_{k-i}] + \sum_{i=N(\delta)+1}^k \mu^i [\Sigma v_{k-i} - v_{k-i}^T \Sigma v_{k-i} v_{k-i}], \end{aligned}$$

and

$$\begin{aligned} \widetilde{M}(v_k) &= \frac{1}{1-\mu} [\Sigma v_k - v_k^T \Sigma v_k v_k] \\ &= \sum_{i=0}^{N(\delta)} \mu^i [\Sigma v_k - v_k^T \Sigma v_k v_k] + \sum_{i=N(\delta)+1}^{\infty} \mu^i [\Sigma v_k - v_k^T \Sigma v_k v_k]. \end{aligned}$$

Note that  $\|v_{k+1} - v_k\| \leq C\eta$ , where  $C = \frac{C_{\delta}}{1-\mu}$  is a constant. Then we have

$$\max_{i=0,1,\dots,N(\eta)} \|v_{k-i} - v_k\| \leq CN(\eta)\eta \rightarrow 0,$$

as  $\eta$  goes to 0. Since  $v$  is bounded, the function  $\Sigma v - v^T \Sigma v v$  is bounded, which implies  $\Sigma v - v^T \Sigma v v$  is Lipschitz. Let  $K$  be the Lipschitz constant. For  $i = 0, 1, \dots, N(\delta)$ , we have

$$\|\Sigma v_k - v_k^T \Sigma v_k v_k - \Sigma v_{k-i} + v_{k-i}^T \Sigma v_{k-i} v_{k-i}\| \leq KCN(\eta)\eta.$$

Then

$$\left\| \sum_{i=0}^{N(\delta)} \mu^i \{[\Sigma v_{k-i} - v_{k-i}^T \Sigma v_{k-i} v_{k-i}] - [\Sigma v_k - v_k^T \Sigma v_k v_k]\} \right\| \leq \frac{KCN(\eta)\eta}{1-\mu}.$$

Since  $\Sigma v_k - v_k^T \Sigma v_k v_k$  is uniformly bounded by  $C$  w.p.1, both  $\sum_{i=N(\delta)+1}^k \mu^i [\Sigma v_{k-i} - v_{k-i}^T \Sigma v_{k-i} v_{k-i}]$  and  $\sum_{i=N(\delta)+1}^{\infty} \mu^i [\Sigma v_k - v_k^T \Sigma v_k v_k]$  are bounded by  $C\eta$ . Thus,

$$\|m_{k+1} - \widetilde{M}(v_k)\| \leq \frac{KCN(\eta)\eta}{1-\mu} + 2C\eta = O(\eta \log \frac{1}{\eta}) \quad w.p.1.$$

For  $k < N(\eta)$ , following the same approach, we can bound  $\|m_{k+1} - \widetilde{M}(v_k)\|$  by the same bound  $O(\eta \log \frac{1}{\eta})$ .  $\square$

### B.3 Proof of Theorem 3.4

*Proof.* Define the sums

$$\begin{aligned}\mathcal{E}^\eta(t) &= \eta \sum_{i=0}^{t/\eta-1} \epsilon_i^\eta, & B^\eta(t) &= \eta \sum_{i=0}^{t/\eta-1} \beta_i^\eta, \\ \bar{G}^\eta(t) &= \eta \sum_{i=0}^{t/\eta-1} \bar{M}(v_i^\eta), & \tilde{G}^\eta(t) &= \eta \sum_{i=0}^{t/\eta-1} [m_{i+1}^\eta - \bar{M}(v_i^\eta)].\end{aligned}$$

Then the algorithm can be written as

$$V^\eta(t) = v_0^\eta + \bar{G}^\eta(t) + \tilde{G}^\eta(t) + B^\eta(t) + \mathcal{E}^\eta(t).$$

Define the process  $W^\eta(t)$  by

$$W^\eta(t) = V^\eta(t) - v_0^\eta - \bar{G}^\eta(t) = \tilde{G}^\eta(t) + B^\eta(t) + \mathcal{E}^\eta(t).$$

First, tightness and Lipschitz continuity of the limit follow from the uniform boundedness of  $v_{k+1}^\eta - v_k^\eta$ . Specifically, there is a subsequence  $\eta(k) \rightarrow 0$  and a process  $V(\cdot)$  such that

$$V^{\eta(k)}(t) \Rightarrow V(t).$$

Here,  $V(t)$  is Lipschitz continuous, which follows from the fact  $\|v_{k+1}^\eta - v_k^\eta\| \leq \frac{C_\delta}{1-\mu}$ . For notational simplicity, we write  $\eta(k)$  as  $\eta$  in the following proof.

For  $t$ , and for integer  $p$ , let  $s_i \leq t$ ,  $i \leq p$ , and  $\tau > 0$ . Let  $f(\cdot)$  be a continuous, bounded and real-valued function. Then by definition of  $W^\eta(t)$ , we have

$$0 = Ef(V^\eta(s_i), i \leq p)[W^\eta(t + \tau) - W^\eta(t)] \tag{B.1}$$

$$- Ef(V^\eta(s_i), i \leq p)[\tilde{G}^\eta(t + \tau) - \tilde{G}^\eta(t)] \tag{B.2}$$

$$- Ef(V^\eta(s_i), i \leq p)[\mathcal{E}^\eta(t + \tau) - \mathcal{E}^\eta(t)] \tag{B.3}$$

$$- Ef(V^\eta(s_i), i \leq p)[B^\eta(t + \tau) - B^\eta(t)]. \tag{B.4}$$

Let  $\mathcal{F}_n^\eta = \sigma\{v_i^\eta, \Sigma_{i-1}, i \leq n\}$ , then  $\mathcal{F}_{t/\eta}^\eta$  measures  $\{\mathcal{E}^\eta(s), s \leq t\}$  by definition and the process  $\mathcal{E}^\eta(\cdot)$  is actually an  $\mathcal{F}_{t/\eta}^\eta$ -martingale. By the tower property of the conditional expectation, we know term (B.3) equals to 0.

Next, we eliminate term (B.4). Note that for any  $m, n > 0$ , we have

$$\left\| \frac{1}{m} \sum_{i=n}^{n+m-1} \mathbb{E}[\beta_i^\eta | \mathcal{F}_n] \right\| = \left\| \frac{1}{m} \sum_{i=n}^{n+m-1} \mu^{i-n} \beta_n^\eta \right\| \leq \frac{1}{(1-\mu)m} \|\beta_n^\eta\|.$$

Since  $\beta_n^\eta$  is uniformly bounded in  $\eta, m$  and  $n$ , we have

$$\lim_{m, n, \eta} \frac{1}{m} \sum_{i=n}^{n+m-1} \mathbb{E}[\beta_i^\eta | \mathcal{F}_n] = 0$$

in  $\mathcal{L}_2$ , which also means

$$\lim_{\eta} \mathbb{E}[B^\eta(t + \tau) - B^\eta(t) | \mathcal{F}_{t/\eta}^\eta] = 0.$$

Together with the boundedness of  $f$ , by Dominated Convergence Theorem, we know that term (B.4) goes to 0, as  $\eta \rightarrow 0$ .

For term (B.2), using Lemma 3.3, we have for any  $\delta > 0$ , when  $\eta$  is small enough,

$$\|\widetilde{G}^\eta(t + \tau) - \widetilde{G}^\eta(t)\| \leq \tau O(\eta \log \frac{1}{\eta}).$$

Thus, term (B.2) goes to 0 as  $\eta \rightarrow 0$ . Then we have

$$\lim_{\eta} E f(V^\eta(s_i), i \leq p) [W^\eta(t + \tau) - W^\eta(t)] = 0.$$

Define

$$W(t) = V(t) - V(0) - \int_0^t \widetilde{M}(V(s)) ds.$$

Then the weak convergence and the previous analysis together imply that

$$E f(V^\eta(s_i), i \leq p) [W(t + \tau) - W(t)] = 0.$$

Here, we need an important result in the martingale theory:

**Theorem B.1** (Kushner and Yin (2003), Theorem 4.1, Chapter 7). *Let  $U(\cdot)$  be a random process with paths in  $D^d[0, \infty)$ , where  $U(t)$  is measurable on the  $\sigma$ -algebra  $\mathcal{F}_t^V$  determined by  $\{V(s), s \leq t\}$  for some given process  $V(\cdot)$  and let  $\mathbb{E}[U(t)] < \infty$  for each  $t$ . Suppose that for each real  $t \geq 0$  and  $\tau \geq 0$ , each integer  $p$  and each set of real numbers  $s_i \leq t$ ,  $i = 1, \dots, p$ , and each bounded and continuous real-valued function  $h(\cdot)$ ,*

$$E h(V^\eta(s_i), i \leq p) [U(t + \tau) - U(t)] = 0,$$

*then  $U(t)$  is a  $\mathcal{F}_t^V$ -martingale.*

By Theorem B.1, we know that  $W(\cdot)$  is a martingale. It has locally Lipschitz continuous sample paths by the fact  $V(\cdot)$  is Lipschitz. Since a Lipschitz continuous martingale must almost surely be a constant, we know  $W(t) = W(0) = 0$  with probability 1. In other words,

$$V(t) = V(0) + \int_0^t \widetilde{M}(V(s)) ds.$$

□

## B.4 Proof of Corollary 3.6

*Proof.* Since all the subsequences have the same limit, by Theorem A.4, we know  $H^\eta(\cdot)$  converges weakly to  $H(\cdot)$ , which means the path  $H^\eta(\cdot)$  closely follows the solution of the ODE on any finite

interval with an arbitrarily high probability as  $\eta \rightarrow 0$ . Note that ODE (3.7) is different from that of VSGD only by a constant  $\frac{1}{1-\mu}$ , and when the initial point is on the sphere  $\mathbb{S}$ , its solution is:

$$H^i(t) = C(t)^{-\frac{1}{2}} H^i(0) \exp\left(\frac{\lambda_i}{1-\mu} t\right), \quad (\text{B.5})$$

where  $C(t) = \sum_i^d (H^i(0) \exp(\frac{\lambda_i}{1-\mu} t))^2$ . When  $\|H(0)\| = 1$  and  $H^1(0) \neq 0$ , this solution  $H(t)$  has been proved in [Chen et al. \(2017\)](#) to converge to the optimal solution  $e_1$ . Thus, the weak convergence of MSGD with random initialization is proved.  $\square$

## C Detailed Proof in Section 4

For notational simplicity, define

$$\Sigma_i = \mathbb{E}[(Y Y^T e_i - e_i^T Y Y^T e_i e_i)(Y Y^T e_i - e_i^T Y Y^T e_i e_i)^T]$$

and

$$\alpha_{i,j} = \sqrt{e_j^T \Sigma_i e_j} = \sqrt{\mathbb{E}[(Y^{(i)})^2 (Y^{(j)})^2]}.$$

### C.1 Proof of Theorem 4.1

*Proof.* The proof follows from Theorem 10.8.1 in [Kushner and Yin \(2003\)](#) (Theorem A.6). We need to check the Assumption A.1 to A.8 (in Appendix A). The uniformly integrability A.1 directly follows from the boundedness property of  $H$ . A.2 can be easily got from the proof of ODE approximation, and A.4 is obviously satisfied since  $e_1$  is the global optimum. Thus, the main challenge here is to calculate the variance of the Wiener process and check the other five assumptions.

For simplicity,  $E_k^\eta F(\xi_{k+j})$  means the conditional expectation for

$$\{\xi_{k+j}, j \geq 0; \xi_k(H) = \xi_k^\eta\}.$$

From Equation (4.2), the variance can be decomposed into three parts. The first part is from the noise  $\gamma_k^{\eta,i}$ . Since we have assumed the weak convergence  $H_k \Rightarrow H^*$ , we have in distribution,

$$\begin{aligned} \lim_{\eta,k} E_k^\eta (\gamma_{k+j}^{\eta,i})^2 &= \lim_{\eta,k} e_i^T E_k^\eta [\gamma_{k+j}^\eta (\gamma_{k+j}^\eta)^T] e_i \\ &= e_i^T \Sigma_1 e_i = \mathbb{E}[Y^{(1)}]^2 (Y^{(j)})^2 = \alpha_{1,i}^2. \end{aligned}$$

Since the limit is a constant, the convergence also holds in probability. Thus, A.5 is satisfied.

The second part comes from the fixed-state-chain:

$$\begin{aligned} E_k^\eta (g^{(i)}(H^*, \xi_{k+j}^\eta(H^*)))^2 &= E_k^\eta (\xi_{k+j}^\eta(H^*))^2 \\ &= \mu^{2j} (\xi_k^{\eta,i})^2 + \sum_{m=0}^{j-1} \mu^{2(j-m)} E_k^\eta [(\Lambda_{k+m} H^* - H^{*T} \Lambda_{k+m} H^* H^*)^{(i)}]^2 \\ &\rightarrow \frac{\mu^2}{1-\mu^2} \alpha_{1,i}^2, \end{aligned}$$

in probability, as  $k, j \rightarrow 0$ . Thus, A.6 is satisfied.

The last part is from the term  $g^{(i)}(\xi_k, H_k) - g^{(i)}(\xi_k(H_k), H_k)$ . Define the discounted sequence

$$\Gamma_k^{\eta, i}(H) = \sum_{j=0}^{\infty} (1-\eta)^j E_k^\eta [g^{(i)}(H, \xi_{k+j}^\eta(H)) - M^{(i)}(H)].$$

Note that

$$\begin{aligned} E_k^\eta [\xi_{k+j}^{\eta, i}(H)] &= E_k^\eta [\mu^j \xi_k^{\eta, i} + (\sum_{m=0}^{j-1} \mu^{j-m} (\Lambda_{k+m} H - H^T \Lambda_{k+m} H H))^{(i)}] \\ &= \mu^j \xi_k^{\eta, i} + (\sum_{m=0}^{j-1} \mu^{j-m} (\Lambda H - H^T \Lambda H H))^{(i)}. \end{aligned}$$

Thus, we have

$$E_k^\eta [g^{(i)}(H, \xi_j^\eta(H)) - M^{(i)}(H)] = \mu^j \xi_k^{\eta, i} - \frac{\mu^{j+1}}{1-\mu} (\Lambda H - H^T \Lambda H H)^{(i)}.$$

Then

$$\Gamma_k^{\eta, i}(H) = \sum_{j=0}^{\infty} (1-\eta)^j \left\{ \mu^j \xi_k^{\eta, i} - \frac{\mu^{j+1}}{1-\mu} (\Lambda H - H^T \Lambda H H)^{(i)} \right\} = \frac{1}{1-(1-\eta)\mu} \left( \xi_k^{\eta, i} - \frac{\mu}{1-\mu} M^{(i)}(H) \right).$$

Since  $M$  is locally Lipschitz, and  $\|h_{k+1}^\eta - h_k^\eta\| = O(\eta)$ , the following result holds:

$$\begin{aligned} \left| E_k^\eta [\Gamma_{k+1}^{\eta, i}(h_{k+1}^\eta) - \Gamma_{k+1}^{\eta, i}(h_k^\eta)] \right|^2 &= \left| \frac{\mu}{(1-(1-\eta)\mu)(1-\mu)} \left\{ E_k^\eta [M^{(i)}(h_{k+1}^\eta) - M^{(i)}(h_k^\eta)] \right\} \right|^2 \\ &= O(\eta^2). \end{aligned}$$

Then, Assumption A.3 holds.

Define another function

$$G_k^{\eta, i}(H, \xi_k^\eta) = E_k^\eta \left[ \Gamma_{k+1}^{\eta, i}(h_k^\eta) Z_k^{\eta, i} \mid h_k^\eta = H \right].$$

It is easy to check this is a continuous function in  $(H, \xi_k^\eta)$ , uniformly in  $k$  and  $\eta$  (Assumption A.7).

Moreover,

$$\begin{aligned} \Gamma_{k+1}^{\eta, i}(h_k^\eta) Z_k^{\eta, i} &= \frac{1}{1-(1-\eta)\mu} \left( \xi_{k+1}^{\eta, i} - \frac{\mu}{1-\mu} M^{(i)}(h_k^\eta) \right) \frac{1}{\mu} \xi_{k+1}^{\eta, i} \\ &= \frac{1}{1-(1-\eta)\mu} \left( \frac{1}{\mu} (\xi_{k+1}^{\eta, i})^2 - \frac{1}{1-\mu} M^{(i)}(h_k^\eta) \xi_{k+1}^{\eta, i} \right). \end{aligned}$$

Then we have

$$\begin{aligned} E_k^\eta [(\xi_{k+1}^{\eta, i})^2 \mid h_k^\eta = H^*] &= E_k^\eta \left[ \left( \mu \xi_k^{\eta, i} + \mu (\Lambda_k h_k^\eta - (h_k^\eta)^T \Lambda_k h_k^\eta h_k^\eta)^{(i)} \right)^2 \mid h_k^\eta = H^* \right] \\ &= \mu^2 (\xi_k^{\eta, i})^2 + \mu^2 \alpha_{i,1}^2, \end{aligned}$$

and

$$E_k^\eta [M^{(i)}(H_k^\eta) \xi_{k+1}^{\eta,i} | H_k^\eta = H^*] = 0.$$

Those imply that

$$\begin{aligned} E_k^\eta G_{k+j}^{\eta,i}(H^*, \xi_{k+j}^\eta(H^*)) &= \frac{\mu}{1 - (1 - \eta)\mu} (E_k^\eta (\xi_{k+j}^\eta(H^*))^2 + \alpha_{i,1}^2) \\ &\rightarrow \frac{1}{1 - \mu^2} \frac{\mu}{1 - \mu} \alpha_{i,1}^2 \end{aligned}$$

in probability. Thus, A.8 is satisfied. We have proved all the assumptions of Theorem A.6 are satisfied. As a result, there exists a Wiener Process  $W$ , such that  $\{U^{\eta,i}\}$  converges weakly to a stationary solution of

$$dU = \frac{(\lambda_i - \lambda_1)}{1 - \mu} U dt + dW, \quad (\text{C.1})$$

where the variance of  $W$  is  $[1 + \frac{\mu^2}{1 - \mu^2} + 2 \frac{1}{1 - \mu^2} \frac{\mu}{1 - \mu}] \alpha_{i,1}^2 = \frac{\alpha_{i,1}^2}{(1 - \mu)^2}$ . Thus, we can also write the above equation as follows:

$$dU = \frac{(\lambda_i - \lambda_1)}{1 - \mu} U dt + \frac{\alpha_{i,1}}{1 - \mu} dB_t. \quad (\text{C.2})$$

□

## C.2 Proof of Lemma 4.2 and Proposition 4.3

*Proof.* Since we restart our record time, we assume here the algorithm is initialized around the global optimum  $e_1$ . Thus, we have  $\sum_{i=2}^d (U^{\eta,i}(0))^2 = \eta^{-1} \delta^2 < \infty$ . Since  $U^{\eta,i}(t)$  approximates to  $U^{(i)}(t)$  in this neighborhood, and the second moment of  $U^{(i)}(t)$  is:

$$\mathbb{E} \left( U^{(i)}(t) \right)^2 = \frac{\alpha_{i,1}^2}{2(1 - \mu)(\lambda_1 - \lambda_i)} + \left( \left( U^{(i)}(0) \right)^2 - \frac{\alpha_{i,1}^2}{2(1 - \mu)(\lambda_1 - \lambda_i)} \right) \exp \left[ -2 \frac{(\lambda_1 - \lambda_i)t}{1 - \mu} \right], \quad \text{for } i \neq 1,$$

by Markov inequality, we have:

$$\begin{aligned} \mathbb{P} \left( \sum_{i=2}^d \left( H_\eta^{(i)}(T_3) \right)^2 > \epsilon \right) &\leq \frac{\mathbb{E} \left( \sum_{i=2}^d \left( H_\eta^{(i)}(T_3) \right)^2 \right)}{\epsilon} = \frac{\mathbb{E} \left( \sum_{i=2}^d \left( U^{\eta,i}(T_3) \right)^2 \right)}{\eta^{-1} \epsilon} \\ &\approx \frac{1}{\eta^{-1} \epsilon} \sum_{i=2}^d \frac{\alpha_{i,1}^2}{2(1 - \mu)(\lambda_1 - \lambda_i)} \left( 1 - \exp \left( -2 \frac{(\lambda_1 - \lambda_i)T_3}{1 - \mu} \right) \right) + \left( U^{\eta,i}(0) \right)^2 \exp \left[ -2 \frac{(\lambda_1 - \lambda_i)T_3}{1 - \mu} \right] \\ &\leq \frac{1}{\eta^{-1} \epsilon} \left( \frac{d \max_{2 \leq i \leq d} (\alpha_{i,1}^2)}{2(1 - \mu)(\lambda_1 - \lambda_2)} \left( 1 - \exp \left( -2 \frac{(\lambda_1 - \lambda_d)T_3}{1 - \mu} \right) \right) + \eta^{-1} \delta^2 \exp \left[ -2 \frac{(\lambda_1 - \lambda_2)T_3}{1 - \mu} \right] \right) \\ &\leq \frac{1}{\eta^{-1} \epsilon} \left( \frac{d \max_{1 \leq i \leq d} (\alpha_{i,1}^2)}{2(1 - \mu)(\lambda_1 - \lambda_2)} + \eta^{-1} \delta^2 \exp \left[ -2 \frac{(\lambda_1 - \lambda_2)T_3}{1 - \mu} \right] \right). \end{aligned}$$

To guarantee  $\frac{1}{\eta^{-1}\epsilon} \left( \frac{d \max_{1 \leq i \leq d} \alpha_{i1}^2}{2(1-\mu)(\lambda_1-\lambda_2)} + \eta^{-1} \delta^2 \exp \left[ -2 \frac{(\lambda_1-\lambda_2)T_3}{1-\mu} \right] \right) \leq \frac{1}{4}$  has a solution, we need:

$$(1-\mu)(\lambda_1-\lambda_2)\epsilon - 2d\eta \max_{1 \leq i \leq d} \alpha_{i1}^2 > 0,$$

which implies Lemma 4.2. Moreover, when the above inequality holds, we have:

$$T_3 = \frac{1-\mu}{2(\lambda_1-\lambda_2)} \log \left( \frac{(1-\mu)(\lambda_1-\lambda_2)\delta^2}{(1-\mu)(\lambda_1-\lambda_2)\epsilon - 2d\eta \max_{1 \leq i \leq d} \alpha_{i1}^2} \right).$$

□

### C.3 Proof of Proposition 4.6

*Proof.* Recall that Theorem 4.5 holds when  $u_k^\eta = (h_k^\eta - e_2)/\sqrt{\eta}$  is bounded. Thus, if  $(H_\eta^{(2)}(T_1))^2 \leq 1 - \delta^2$  holds at some time  $T_1$ , the algorithm has successfully escaped the saddle point. We approximate  $U^{\eta,1}(t)$  by the limiting process approximation, which is normal distributed at time  $t$ . As  $\eta \rightarrow 0$ , by simple manipulation, we have

$$\mathbb{P}\left((H^{\eta,2}(T_1))^2 \leq 1 - \delta^2\right) = \mathbb{P}\left((U^{\eta,2}(T_1))^2 \leq \eta^{-1}(1 - \delta^2)\right).$$

We then prove  $P\left(|U^{\eta,1}(T_1)| \geq \eta^{-\frac{1}{2}}\delta\right) \geq 1 - \nu$ . At time  $t$ ,  $U^{\eta,1}(t)$  approximates to a normal distribution with mean 0 and variance  $\frac{\alpha_{12}^2}{2(1-\mu)(\lambda_1-\lambda_2)} \left[ \exp\left(2 \frac{(\lambda_1-\lambda_2)T_1}{1-\mu}\right) - 1 \right]$ . Therefore, let  $\Phi(x)$  be the CDF of  $N(0,1)$ , we have

$$\mathbb{P} \left( \frac{|U^{\eta,1}(T_1)|}{\sqrt{\frac{\alpha_{12}^2}{2(1-\mu)(\lambda_1-\lambda_2)} \left[ \exp\left(2 \frac{(\lambda_1-\lambda_2)T_1}{1-\mu}\right) - 1 \right]}} \geq \Phi^{-1}\left(\frac{1+\nu}{2}\right) \right) \approx 1 - \nu,$$

which requires

$$\eta^{-\frac{1}{2}}\delta \leq \Phi^{-1}\left(\frac{1+\nu}{2}\right) \cdot \sqrt{\frac{\alpha_{12}^2}{2(1-\mu)(\lambda_1-\lambda_2)} \left[ \exp\left(2 \frac{(\lambda_1-\lambda_2)T_1}{1-\mu}\right) - 1 \right]}.$$

Solving the above inequality, we get

$$T_1 = \frac{(1-\mu)}{2(\lambda_1-\lambda_2)} \log \left( \frac{2\eta^{-1}\delta^2(1-\mu)(\lambda_1-\lambda_2)}{\Phi^{-1}\left(\frac{1+\nu}{2}\right)^2 \alpha_{12}^2} + 1 \right).$$

□

### C.4 Proof of Proposition 4.4

*Proof.* After Phase I, we restart our record time, i.e.,  $H^{\eta,1}(0) = \delta$ . By Corollary 3.6, we obtain

$$\begin{aligned} (H^{\eta,1}(T_2))^2 &\approx (H^{(1)}(T_2))^2 = \left( \sum_{j=1}^d \left( (H^{(j)}(0))^2 \exp\left(2\frac{\lambda_j}{1-\mu} T_2\right) \right) \right)^{-1} (H^{(1)}(0))^2 \exp\left(2\frac{\lambda_1}{1-\mu} T_2\right) \\ &\geq \left( \delta^2 \exp\left(2\frac{\lambda_1}{1-\mu} T_2\right) + (1-\delta^2) \exp\left(2\frac{\lambda_2}{1-\mu} T_2\right) \right)^{-1} \delta^2 \exp\left(2\frac{\lambda_2}{1-\mu} T_2\right), \end{aligned}$$

which requires

$$\left( \delta^2 \exp\left(2\frac{\lambda_1}{1-\mu} T_2\right) + (1-\delta^2) \exp\left(2\frac{\lambda_2}{1-\mu} T_2\right) \right)^{-1} \delta^2 \exp\left(2\frac{\lambda_1}{1-\mu} T_2\right) \geq \eta^{-1}(1-\delta^2).$$

Solving the above inequality, we get

$$T_2 = \frac{1-\mu}{2(\lambda_1-\lambda_2)} \log \frac{1-\delta^2}{\delta^2}.$$

□

## D Deep Neural Networks Experiments

| Experiment 1   |      |      |      |      |      |      |
|----------------|------|------|------|------|------|------|
| initial $\mu$  | 0    |      |      | 0.9  |      |      |
| initial $\eta$ | 0.05 | 0.02 | 0.01 | 0.05 | 0.02 | 0.01 |
| Experiment 2   |      |      |      |      |      |      |
| initial $\mu$  | 0    |      |      | 0.9  |      |      |
| initial $\eta$ | 0.5  | 0.2  | 0.1  | 0.05 | 0.02 | 0.01 |
| Experiment 3   |      |      |      |      |      |      |
| initial $\mu$  | 0    |      |      | 0.9  |      |      |
| initial $\eta$ | 1    | 0.5  | 0.2  | 0.5  | 0.2  | 0.1  |

Table 1: Our Settings in each Experiment. For VSGD, we set  $\mu = 0$ ; for MSGD we set  $\mu = 0.9$ .

| layer name | output size    | 18 layers   |
|------------|----------------|---|
| Conv1      | $32 \times 32$ | $[3 \times 3, 32] \times 3$ , stride 1                                      |
| Conv2.x    | $32 \times 32$ | $\begin{bmatrix} 3 \times 3, 32 \\ 3 \times 3, 32 \end{bmatrix} \times 3$   |
| Conv3.x    | $16 \times 16$ | $[3 \times 3, 64] \times 1$ , stride 2                                      |
| Conv4.x    | $16 \times 16$ | $\begin{bmatrix} 3 \times 3, 64 \\ 3 \times 3, 64 \end{bmatrix} \times 3$   |
| Conv5.x    | $8 \times 8$   | $[3 \times 3, 128] \times 1$ , stride 2                                     |
| Conv6.x    | $8 \times 8$   | $\begin{bmatrix} 3 \times 3, 128 \\ 3 \times 3, 128 \end{bmatrix} \times 3$ |
|            | $1 \times 1$   | average pooling, 1000-d fc, softmax   |

Table 2: Our Network Architecture. Conv2.x, Conv3.x, Conv4.x, Conv5.x, and Conv6.x denote convolution units that may contain multiple convolution layers. E.g.,  $[3 \times 3, 64] \times 3$  denotes 3 cascaded convolution layers with 64 filters of size  $3 \times 3$ . Also we train our neural network with Sphere-Corr [Liu et al. \(2017\)](#).